

Weierstraß-Institut für Angewandte Analysis und Stochastik

im Forschungsverbund Berlin e.V.

Preprint

ISSN 0946 – 8633

Determination of stiffness and higher gradient coefficients by means of the embedded atom method: An approach for binary alloys

Thomas Böhme ¹ , Wolfgang Dreyer ² , Wolfgang H. Müller¹

submitted: 8th May 2006

¹ Institut für Mechnaik,
LKM, Sekr. MS-2,
Technische Universität Berlin,
Einsteinufer 5, D-10587 Berlin,
Germany
E-Mail: thomas.boehme@tu-berlin.de,
wolfgang.h.mueller@tu-berlin.de

² Weierstrass Institut
für Angewandte Analysis und Stochastik,
Mohrenstraße 39, D-10119 Berlin,
Germany,
E-Mail: dreyer@wias-berlin.de

No. 1131

Berlin 2006



2000 *Mathematics Subject Classification.* 74A15, 74N05, 74N25, 82B20, 82B26.

Key words and phrases. atomic potentials, crystals, elastic constants, higher gradient coefficients, phase diagram, diffusion, phase transformation, phase field theories.

Edited by
Weierstraß-Institut für Angewandte Analysis und Stochastik (WIAS)
Mohrenstraße 39
10117 Berlin
Germany

Fax: + 49 30 2044975
E-Mail: preprint@wias-berlin.de
World Wide Web: <http://www.wias-berlin.de/>

Abstract

For a quantitative theoretical description of phase separation and coarsening reliable data of stiffness constants and the so called Higher Gradient Coefficients (HGCs) are required. For that reason pair potentials of the Lennard-Jones type were used in [1] to provide a theoretical tool for their quantitative determination. Following up on this work these quantities are now calculated by means of the Embedded-Atom Method (EAM), a recently developed approach to describe interatomic potentials in metals. This is done, first, to achieve a better agreement between predicted and experimentally observed stiffness data as well as to avoid artifacts, such as the Cauchy paradox, and, second, to increase the trustworthiness of the HGCs for which experimental data are rarely available. After an introduction to the fundamentals of EAM it is outlined how it can be used for calculating stiffness constants and HGCs. In particular, Johnson's modification of EAM for nearest neighbor interactions [3] is applied to present explicit numerical results for a case study alloy, Ag-Cu, which has a "simpleface-centered-cubic crystal structure and where it is comparatively easy to obtain all the required analysis data from the literature and to experimentally compare the predictions of mechanical data.

1 Introduction

The theoretical description of phase separation as a consequence of spinodal decomposition or nucleation and subsequent coarsening (Ostwald ripening) is a widely spread and ongoing research area. Originally this form of solid-solid phase transformation was effectively described in the seminal papers of Cahn and Hilliard [6] and Cahn [7]. They used so called phase field theories and derived a diffusion equation that, for the first time, allowed a qualitative description of phase separation phenomena ("uphill" diffusion). Since then phase field theories were the objects of numerous research groups and investigated from different points of view (e.g., [8], [9] or [10]).

In [2] Dreyer and Müller presented an approach for the theoretical description of phase separation in binary alloys triggered by spinodal decomposition and followed by coarsening. It is based on the evaluation of the dissipation inequality by methods of Rational Thermodynamics. As a result of their considerations an extended diffusion equation was formulated representing a generalization of the well-known Cahn-Hilliard equation [11]. It reads:

$$\rho_0 \frac{\partial c}{\partial t} + \frac{\partial J_i}{\partial X_i} = 0 \quad (\text{mass balance}). \quad (1)$$

Here $c = \tilde{c}(X_i, t)$ represents the mass concentration in the material as a function of reference position X_i and time t . Furthermore ρ_0 is the mass density of the alloy in its (liquid) reference state. The (extended) diffusion flux J_i combines the influences of concentration gradients, surface

tensions, and mechanical strains and can be written as follows (cf., Appendix A):

$$J_i = - \rho_0 M_{ij} \frac{\partial}{\partial X_j} \left(\frac{\partial \psi_0}{\partial c} - 2A_{kl} \frac{\partial^2 c}{\partial X_k \partial X_l} - \frac{\partial A_{kl}}{\partial c} \frac{\partial c}{\partial X_k} \frac{\partial c}{\partial X_l} - 2 \frac{\partial A_{kl}}{\partial \varepsilon_{mn}} \frac{\partial c}{\partial X_k} \frac{\partial \varepsilon_{mn}}{\partial X_l} - \frac{\partial^2 a_{kl}}{\partial \varepsilon_{op} \partial \varepsilon_{mn}} \frac{\partial \varepsilon_{op}}{\partial X_k} \frac{\partial \varepsilon_{mn}}{\partial X_l} - \frac{\partial a_{kl}}{\partial \varepsilon_{mn}} \frac{\partial^2 \varepsilon_{mn}}{\partial X_k \partial X_l} \right). \quad (2)$$

The symbol M_{ij} denotes the mobility matrix and can be linked to diffusion coefficients commonly used in Fick's first law, $\psi_0 = \tilde{\psi}_0(c, T, \varepsilon_{kl})$ stands for the Gibbs free energy of an equivalent homogeneous system with mass concentration c , and $a_{kl} = \tilde{a}_{kl}(c, T, \varepsilon_{kl})$, $b_{kl} = \tilde{b}_{kl}(c, T, \varepsilon_{kl})$, and $A_{kl} = \frac{\partial a_{kl}}{\partial c} + b_{kl}$ being the so-called Higher Gradient Coefficients (HGCs) taking concentration gradients into account.

For a *quantitative* assessment of the diffusion process realistic material data are required, i.e., in particular the material parameters *of the binary mixture* ρ_0 , M_{ij} , ψ_0 , A_{kl} , a_{kl} , b_{kl} and C_{klmn} must be specified. Note that, for a prescribed external load, the stiffness constants C_{klmn} are, in the simplest case, combined with the strains ε_{kl} according to Hooke's law.

In the present paper we consider a binary alloy A-B below its critical temperature (melting point). Usually such systems consist of two or more phases, which differ in their composition, i.e., in the concentrations of the components c_A or $c_B = (1 - c_A)$, respectively. For instance in pure solid mixtures below the eutectic temperature one can observe two different phases, the α -phase (A-rich) with the equilibrium concentration c_α and the β -phase (B-rich) with c_β , cf., Figure 1. Furthermore phase field theories are characterized by "smooth interfaces between the α - and β -phases (in contradiction to sharp interfaces), i.e., a phase boundary allowing for a continuous change between the equilibrium concentrations c_α and c_β . Therefore it is reasonable to concentrate on the material data of, first, the α -phase, second, the β -phase and, third, of the phase boundary.

The aim of this paper is providing a theoretical approach for the determination of the stiffness C_{klmn} and the higher gradient coefficients a_{kl} , b_{kl} and A_{kl} of the different phases in binary alloys below T_{eut} . This is particularly useful in the case of the HGCs since there is a considerable lack of data in literature. The approach is based on the evaluation of interatomic potentials and allows for a quantitative calculation of these material data in order to perform computer simulations based on the equations (1-2). With respect to the material data within the phase boundary a linear interpolation as follows:

$$\Xi(c) = \Theta(c)\Xi_\alpha + (1 - \Theta(c))\Xi_\beta \quad , \quad \Theta(c) = \frac{c_\beta - c}{c_\beta - c_\alpha} \quad (\text{shape function}) \quad , \quad (3)$$

between the material data $\Xi_\alpha = \{C_{klmn}^\alpha, A_{kl}^\alpha, a_{kl}^\alpha\}$ and $\Xi_\beta = \{C_{klmn}^\beta, A_{kl}^\beta, a_{kl}^\beta\}$ of the equilibrium phases can be performed. Consequently it only remains to specify $\Xi_{\alpha/\beta}$. However, this linear

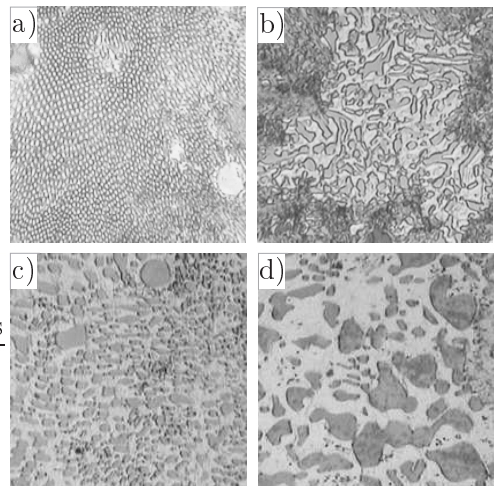


Figure 1: Spinodal decomposition in eutectic Ag-Cu after various heat treatments at 1000 K; a) 0h, b) 5h, c) 20h and d) 40h; dark: Cu-rich (β), light: Ag-rich (α), scale: 1:1000

approach represents only a first approximation, and it is more desirable to find the general dependence $\Xi = \tilde{\Xi}(c)$. Then the interpolation of Eq (3) becomes redundant.

Atomistic arguments for the calculation of stiffness coefficients as well as higher gradient coefficients of Ag-Cu have already been presented by Dreyer and Müller in [1]. However, problems arose already during the prediction of the stiffness constants of the pure substances, C_{klmn}^{Ag} and C_{klmn}^{Cu} , respectively. Due to the use of pair potentials (Lennard-Jones potentials) the Cauchy paradox ($C_{1122} = C_{2323}$) could a priori not be avoided and, consequently, the deviation from experimental data was considerable. Moreover, for alloys showing a higher degree of anisotropy than cubic crystal structure (e.g., Sn-Pb, BCT-structure) negative shear moduli were obtained, [1].

Consequently the predicted HGCs seemed also questionable and alternative atomistic methods should be used that avoid the aforementioned shortcomings. The Embedded-Atom Method (EAM) is such a technique. It is a powerful, semi-empirical approach that allows to capture the state of energy of an atomic system reasonably well. It was developed in the eighties by Daw and Baskes, [12] and [13], and considerably improves the quality of data when predicting physical properties of alloys, especially for those of the FCC type.

In the following section we want to give a brief introduction to the general idea of EAM and to the underlying assumptions. After that we concentrate on the analytic EAM-model proposed by Johnson, [3], which holds for nearest neighbor interactions. It is shown how the expression for the energy can be evaluated for binary alloys to obtain atomistic relations for the stiffness and the higher gradient coefficients. In the last part of the paper we consider the brazing binary alloy Ag-Cu, which has a simple FCC-structure. In particular, we illustrate the fitting procedure and present results with respect to the elastic constants and HGCs. Finally we construct the solid part of the phase diagram in order to emphasize the trustworthiness of the predicted values.

2 Introduction to EAM

2.1 Basic concepts of EAM

The principle of EAM is illustrated in Figure 2. If effects of lattice dynamics are ignored the energy of a solid is exclusively given by *static* atomic interactions. Unlike during the use of pair-potentials¹ the mathematical key to EAM consists of introducing a nonlinear function $F_\alpha = \tilde{F}_\alpha(\bar{\rho}_\alpha)$ in the energy expression for atom α , *in addition* to the pairwise-interaction term:

$$E_\alpha = \frac{1}{2} \sum_{\substack{\beta \\ (\beta \neq \alpha)}} \phi^{\alpha\beta}(r^{\alpha\beta}) + F_\alpha(\bar{\rho}_\alpha) \quad \text{where} \quad \bar{\rho}_\alpha = \sum_{\substack{\beta \\ (\beta \neq \alpha)}} \rho_\beta(r^{\alpha\beta}). \quad (4)$$

F_α is known as the embedding function and $\bar{\rho}_\alpha$ is the (constant) electron density at the position r_i^α of atom α due to all neighbors β . The first term in (4)₁ refers to interactions between the nuclei and the second to atom-electron interactions. This type of separation was proposed by Daw and Baskes and can be justified by quantum-mechanical arguments [12, 13]. The contribution to the electron density by the neighbor β , ρ_β , is a function of the scalar distance $r^{\alpha\beta}$ between atom α

¹Here the energy E_α of a particle (atom) α is given by $E_\alpha = \frac{1}{2} \sum_{\beta(\alpha \neq \beta)} \varphi^{\alpha\beta}(r^{\alpha\beta})$, where $\varphi^{\alpha\beta}$ denotes the pairwise interaction potential between the atoms α and β and depends only upon the radial distance $r^{\alpha\beta}$ between α and β .

and the nucleus of β . Summation of the contributions from all neighbors yields $\bar{\rho}_\alpha$, which can be interpreted as a constant background electron density of a homogeneous electron gas. Thus $\bar{\rho}_\alpha$ denotes the resulting electron density, which is “felt” by atom α due to the presence of its neighbors β .

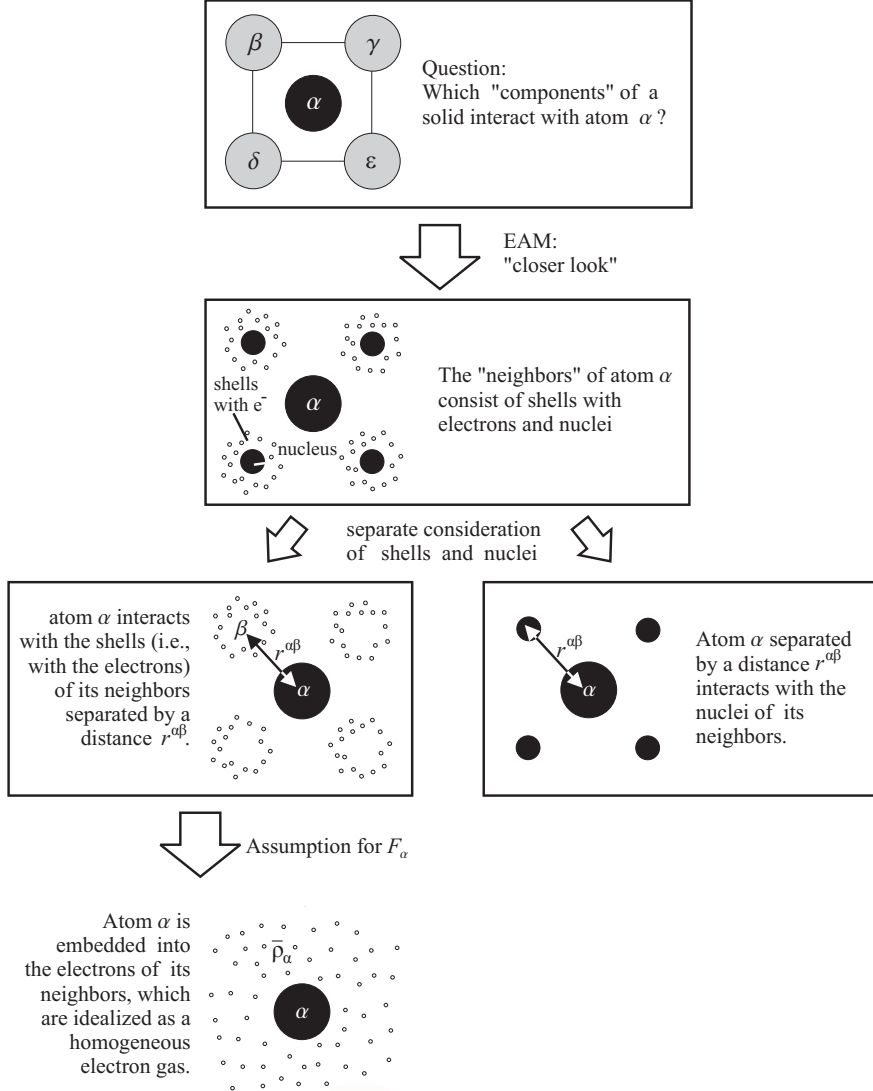


Figure 2: The general principle of the EAM as proposed by Daw and Baskes [12, 13]

The embedding function, $F_\alpha(\bar{\rho}_\alpha)$, can be interpreted as the energy required to incorporate an atom α in a homogeneous electron gas with the constant electron density $\bar{\rho}_\alpha$. Note that the functional form of F_α depends only on the type of the (embedded) atom α and the argument of F_α refers to the electron density of the medium in which atom α is embedded.

$\phi^{\alpha\beta} = \tilde{\phi}^{\alpha\beta}(r^{\alpha\beta})$ characterizes the (purely repulsive) interactions between the nuclei of atom α and β . It depends on the scalar distance $r^{\alpha\beta}$ between α and β and is, according to [3], a positive, monotonically decreasing function.

In summary we may say that in order to determine the energy E_α of a particle α in a binary alloy A-B it is required to know the following quantities: F_A , F_B , ρ_A , ρ_B , ϕ^{AA} , ϕ^{BB} , and ϕ^{AB} . With the exception of ϕ^{AB} all of these functions can easily be related to (macroscopic) mechanical and calorimetric data of the pure substances A and B. In order to obtain ϕ^{AB} a model will be used that relates this quantity to the interactions ϕ^{AA} and ϕ^{BB} of the pure substances.

In the following sections it is assumed that every atom in the solid interacts only with its nearest neighbors (first shell). This assumption leads to a special modification of EAM introduced by Johnson in [3].

2.2 Johnson's analytic nearest-neighbor model

Consider Figure 3 and recall that in an FCC-lattice an arbitrary atom α is surrounded by exactly twelve nearest neighbors from which it is separated by the distance $r^{\alpha\beta} \equiv r = a/\sqrt{2}$ (or, in equilibrium, $R = a_e/\sqrt{2}$), where a denotes the lattice parameter.

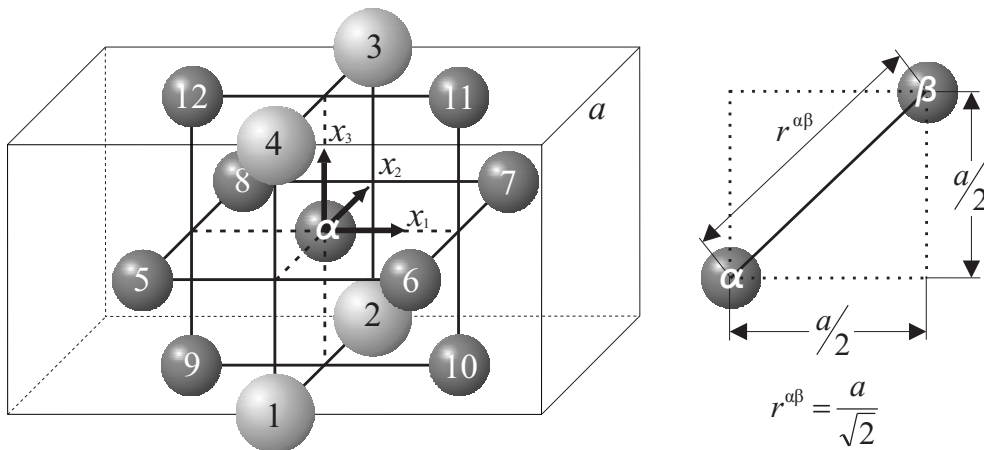


Figure 3: The nearest neighbors for an arbitrary atom α in a FCC-lattice

In order to obtain E_α in Eq (4) it is necessary to specify $\phi^{\alpha\beta}$, F_α and $\rho_\beta (\Rightarrow \bar{\rho}_\alpha)$. More specifically we have to choose a suitable functional form. In particular for a binary alloy A-B the functions F_A , F_B , ρ_A , ρ_B , ϕ^{AA} , ϕ^{BB} , and ϕ^{AB} must be specified. For that reason Johnson proposed in [3] to use the following form² for $\rho_{A/B}$ and $\phi^{AA/BB}$ (where the indices A and B of the two atom species have been omitted for simplicity):

$$\rho(r) = \rho_e \exp \left[-\beta \left(\frac{r}{R} - 1 \right) \right] \quad , \quad \phi(r) = \phi_e \exp \left[-\gamma \left(\frac{r}{R} - 1 \right) \right]. \quad (5)$$

The four parameters ρ_e , ϕ_e , β , and γ depend on the type of the atom and will be determined using information from both pure substances, A and B. Furthermore the nearest neighbor distance R must be known or calculated from the lattice parameter a_e as indicated before.

For the interaction ϕ^{AB} between nuclei of different atom types Johnson used the following form:

$$\phi^{AB}(r) = \frac{1}{2} \left[\frac{\rho_B(r)}{\rho_A(r)} \phi^{AA}(r) + \frac{\rho_A(r)}{\rho_B(r)} \phi^{BB}(r) \right]. \quad (6)$$

²Especially the form of the atomic electron density ρ is borrowed from atoms with isotropic s-orbitals. This (for special cases) unrealistic assumption is later corrected by the fitting procedure.

This relation can easily be quantified using data for the pure substances A and B.

Finally it remains to specify F_A and F_B . For this purpose a universal function of state is used as suggested by Rose et al. [14]. According to them the particle-specific energy for a broad range of materials can be approximated by:

$$E(a) = -E_{\text{sub}}[1 + a^*(a)]e^{-a^*(a)} \quad , \quad a^*(a) = \left(\frac{a}{a_e} - 1\right) \left(\frac{E_{\text{sub}}}{9\kappa\Omega_0}\right)^{-\frac{1}{2}} \quad , \quad (7)$$

where E_{sub} denotes the sublimation energy per atom of the material, κ is the compressibility and Ω_0 is the volume occupied by an atom in the lattice at equilibrium. Hence Ω_0 is a function of a_e and, for an FCC-lattice, can be obtained from:

$$\Omega_0 = \frac{a_e^3}{4} \quad , \quad (8)$$

because there are four atoms in the unit cell ($8 \times \frac{1}{8}$ atoms in the corner; $6 \times \frac{1}{2}$ atoms on the faces). All quantities in Eq (7) can be found in the literature or databases, e.g., [15].

By combining the relation $E(a) = E_\alpha$ with Eq (4) and substituting $a = r\sqrt{2}$ and $a_e = R\sqrt{2}$ by the inverse relation resulting from Eq (5), namely:

$$\ln \frac{\bar{\rho}}{\bar{\rho}_e} = -\beta \left(\frac{r}{R} - 1\right) \quad , \quad \frac{\phi}{\phi_e} = \left(\frac{\bar{\rho}}{\bar{\rho}_e}\right)^{\frac{\gamma}{\beta}} \quad (9)$$

the following form is obtained for F :

$$F(\bar{\rho}) = -E_{\text{sub}} \left[1 - \frac{\alpha}{\beta} \ln \left(\frac{\bar{\rho}}{\bar{\rho}_e}\right)\right] \left(\frac{\bar{\rho}}{\bar{\rho}_e}\right)^{\frac{\alpha}{\beta}} - 6\phi_e \left(\frac{\bar{\rho}}{\bar{\rho}_e}\right)^{\frac{\gamma}{\beta}} \quad \text{and} \quad \alpha = 3 \left(\frac{\kappa\Omega_0}{E_{\text{sub}}}\right)^{\frac{1}{2}} \quad . \quad (10)$$

For this result the relations:

$$\bar{\rho}(r) = \sum_{\beta} \rho(r) = 12\rho(r) \quad , \quad \frac{1}{2} \sum_{\beta} \phi(r) = \frac{1}{2} 12\phi(r) = 6\phi(r) \quad (11)$$

were used which hold for FCC crystals and nearest-neighbor-interactions. Note that the explicit form of $F = \tilde{F}(\bar{\rho})$ only arises because of the special functional forms in Eq (5), which allow an inversion from r to $\bar{\rho}$.

In order to determine all relevant functions for a binary alloy in Eq (4) it is necessary to know the various material parameters introduced in Eqns (5) and (10), namely α , β , γ , ϕ_e , and $\bar{\rho}_e = 12\rho_e$ for the pure substances A and B. How to obtain these quantities through a fitting procedure will be explained in one of the following sections.

3 Evaluation of the EAM energy expression

3.1 Lattice deformation and strain measures

We consider an arbitrary lattice, where the equilibrium state is denoted by the undeformed (reference) configuration. In this case the position of an arbitrary atom α is given by its reference position vector X_i^α . Analogously the atom of the deformed lattice configuration beyond the

equilibrium is characterized by the current position vector $x_i^\alpha = X_i^\alpha + \xi_i^\alpha$, where ξ_i^α denotes the displacement of atom α from his reference position. In the same manner all lattice atoms $\beta, \gamma, \delta, \dots$ are characterized, i.e., the conglomerate of all reference positions $(X_i^\alpha, X_i^\beta, X_i^\gamma, \dots)$ and current positions $(x_i^\alpha, x_i^\beta, x_i^\gamma, \dots)$ contains the whole information about the undeformed or deformed lattice, respectively. Moreover, the distance between two arbitrary atoms α and β is written as $R_i^{\alpha\beta} \equiv X_i^\beta - X_i^\alpha$ or $r_i^{\alpha\beta} \equiv x_i^\beta - x_i^\alpha$ (also note Figure 4 for an illustration of the situation. Consequently the following relations can easily be obtained:

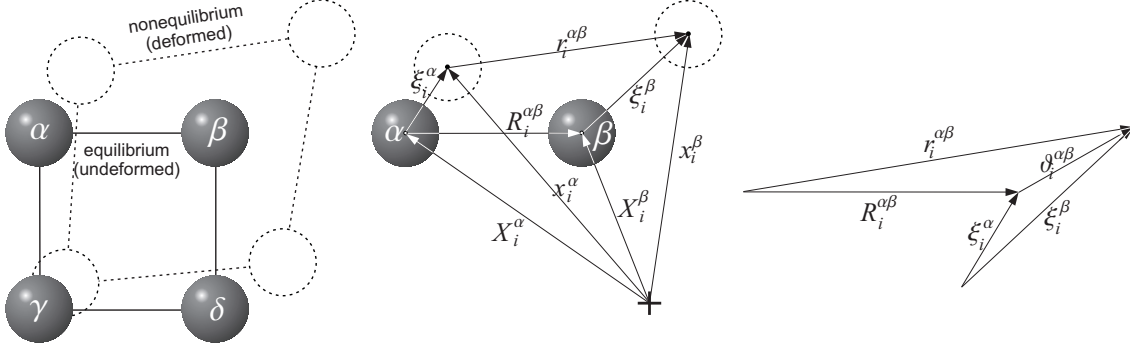


Figure 4: The different lattice vectors and their notation

$$x_i^\alpha = X_i^\alpha + \xi_i^\alpha, \quad x_i^\beta = X_i^\beta + \xi_i^\beta, \quad (12)$$

$$r_i^{\alpha\beta} = x_i^\beta - x_i^\alpha = X_i^\beta - X_i^\alpha + \xi_i^\beta - \xi_i^\alpha = R_i^{\alpha\beta} + \xi_i^\beta - \xi_i^\alpha. \quad (13)$$

By performing the so called *mean field limit*, i.e., by introducing a continuous displacement function $u_i = \tilde{u}_i(X_j^\alpha)$ instead of the discrete displacements ξ_i^α , a Taylor expansion [1] yields:

$$\xi_i^\alpha = u_i(X_j^\alpha) \equiv u_i(X_j), \quad (14)$$

$$\xi_i^\beta = u_i(X_j^\beta) = u_i(X_j^\alpha + R_j^{\alpha\beta}) = u_i(X_j) + \frac{\partial u_i}{\partial X_j} R_j^{\alpha\beta} + \dots, \quad (15)$$

$$\Rightarrow r_i^{\alpha\beta} = R_i^{\alpha\beta} + \frac{\partial u_i}{\partial X_j} R_j^{\alpha\beta} = (\delta_{ij} + H_{ij}) R_j^{\alpha\beta} \equiv F_{ij} R_j^{\alpha\beta}. \quad (16)$$

Here $F_{ij} = \delta_{ij} + H_{ij}$ denotes the coefficients of the deformation gradient and $H_{ij} = \frac{\partial u_i}{\partial X_j}$ stands for coefficients of the displacement gradient.

In order to identify the elastic constants in atomistic theories numerous publications based on interatomic interactions (e.g., two-body atom-atom interactions) can be found, e.g., [4, 5]. Usually the authors consider the total energy of the N (deformed) lattice bonds, $\Phi(r_i^1, \dots, r_i^N)$, as a function of the current distance vector between the atoms and expand the energy in a Taylor series as follows, [4]:

$$\begin{aligned} \Phi(r_i^1, \dots, r_i^N) &= \Phi(R_i^1 + H_{ij} R_j^1, \dots, R_i^N + H_{ij} R_j^N) \\ &= \Phi(R_i^1, \dots, R_i^N) + \sum_b \frac{\partial \Phi}{\partial r_j^b} \Big|_{R_j^b} \vartheta_j^b + \frac{1}{2} \sum_b \frac{\partial^2 \Phi}{\partial r_k^b \partial r_l^b} \Big|_{R_k^b, R_l^b} \vartheta_k^b \vartheta_l^b + \dots \quad (17) \end{aligned}$$

In this equation the index b identifies the bond between the different atoms α and β and the symbol ϑ_i^b denotes the coefficients of the difference vector of the displacements of α and β , namely

$\xi_i^\beta - \xi_i^\alpha \approx \frac{\partial u_i}{\partial X_j} R_j^{\alpha\beta}$ according to $\vartheta_i^{\alpha\beta}$ in Figure 4. Thus Eq (17) can be reformulated as:

$$\begin{aligned} \Phi(r_i^1, \dots, r_i^N) &= \Phi(R_i^1, \dots, R_i^N) + \\ &+ H_{ij} \sum_b \frac{\partial \Phi}{\partial r_i^{\alpha\beta}} \Big|_{R_i^{\alpha\beta}} R_j^{\alpha\beta} + \frac{1}{2} H_{ij} H_{kl} \sum_b \frac{\partial^2 \Phi}{\partial r_j^{\alpha\beta} \partial r_l^{\alpha\beta}} \Big|_{R_j^{\alpha\beta}, R_l^{\alpha\beta}} R_i^{\alpha\beta} R_k^{\alpha\beta}. \end{aligned} \quad (18)$$

The first derivatives of Φ vanish at equilibrium. Therefore the total elastic energy of the lattice is represented by the second-derivative-term of Eq (18). Substituting H_{ij} by its symmetric part, the coefficients of the strain tensor ε_{ij} , this term can be linked to the stiffness coefficients C_{ijkl} , [5].

Unfortunately we could not find a completely convincing argument justifying the substitution $H_{ij} \rightarrow \varepsilon_{ij}$ and hence we want to use another strain measure in order to avoid further irritations and misunderstandings. For this purpose we consider the square of Eq (16):

$$\begin{aligned} r^{\alpha\beta^2} &= r_i^{\alpha\beta} r_i^{\alpha\beta} = F_{ij} F_{ik} R_j^{\alpha\beta} R_k^{\alpha\beta} = C_{jk} R_j^{\alpha\beta} R_k^{\alpha\beta} = R^{\alpha\beta^2} + (C_{jk} - \delta_{jk}) R_j^{\alpha\beta} R_k^{\alpha\beta} \\ &= R^{\alpha\beta^2} + 2G_{jk} R_j^{\alpha\beta} R_k^{\alpha\beta}, \end{aligned} \quad (19)$$

where $C_{jk} = F_{ij} F_{ik} \equiv \mathbf{F}^T \cdot \mathbf{F}$ stands for the right Cauchy-Green tensor and $G_{jk} = \frac{1}{2}(C_{jk} - \delta_{jk}) \equiv \frac{1}{2}(\mathbf{C} - \mathbf{I})$ for Green's strain tensor. By means of G_{jk} we can write for the energy of a lattice:

$$\begin{aligned} \Phi(r^{\alpha\beta^2}) &= \Phi(R^{\alpha\beta^2} + 2G_{jk} R_j^{\alpha\beta} R_k^{\alpha\beta}) = \Phi(R^{\alpha\beta^2}) + \\ &+ 2G_{ij} \sum_b \frac{\partial \Phi}{\partial r^{\alpha\beta^2}} \Big|_{R^{\alpha\beta^2}} R_i^{\alpha\beta} R_j^{\alpha\beta} + \frac{4}{2} G_{ij} G_{kl} \sum_b \frac{\partial^2 \Phi}{\partial r^{\alpha\beta^2} \partial r^{\alpha\beta^2}} \Big|_{R^{\alpha\beta^2}} R_i^{\alpha\beta} R_j^{\alpha\beta} R_k^{\alpha\beta} R_l^{\alpha\beta} + \dots \end{aligned} \quad (20)$$

This equation can be linked to the stiffness coefficients without any further substitutions. However, the underlying interatomic potentials have to be reformulated in terms of $r^{\alpha\beta^2}$.

3.2 Equilibrium condition and stiffness coefficients

According to Section 2 the EAM energy expression of the *whole* system is given by the sum of the energies of all atoms in the system, $E_{\text{tot}} = \sum_{\alpha} E_{\alpha}$, where E_{α} is given by Eq (4). Because $\phi^{\alpha\beta}$, ρ_{β} and $\bar{\rho}_{\alpha}$ only depend on the scalar distance $r^{\alpha\beta}$ between α and β it is also possible to use $r^{\alpha\beta^2}$ for the argument. The corresponding functions are $\hat{\phi} = \tilde{\phi}(r^{\alpha\beta^2})$ and $\hat{\rho}_{\beta} = \tilde{\rho}_{\beta}(r^{\alpha\beta^2})$ and one can write:

$$E_{\text{tot}} = \sum_{\alpha} E_{\alpha} = \frac{1}{2} \sum_{\substack{\alpha, \beta \\ (\beta \neq \alpha)}} \hat{\phi}^{\alpha\beta}(r^{\alpha\beta^2}) + \sum_{\alpha} \hat{F}_{\alpha}(\hat{\rho}_{\alpha}) \quad \text{and} \quad \hat{\rho}_{\alpha} = \sum_{\substack{\beta \\ (\beta \neq \alpha)}} \hat{\rho}_{\beta}(r^{\alpha\beta^2}). \quad (4a)$$

For convenience we will omit the circumflexes $\hat{}$ in the following sections. $\phi^{\alpha\beta}$, ρ_{β} and $\bar{\rho}_{\alpha}$ are implicitly referred to the argument $r^{\alpha\beta^2}$. The individual energy contributions of Eq (4a) can be expanded in a Taylor series at equilibrium (undeformed state). The following steps seem worth mentioning:

$$\begin{aligned} \phi^{\alpha\beta}(r^{\alpha\beta^2}) &= \phi^{\alpha\beta}(R^{\alpha\beta^2} + 2G_{ij} R_i^{\alpha\beta} R_j^{\alpha\beta}) = \\ &= \phi^{\alpha\beta}(R^{\alpha\beta^2}) + 2\phi^{\alpha\beta'}(R^{\alpha\beta^2}) G_{ij} R_i^{\alpha\beta} R_j^{\alpha\beta} + 2\phi^{\alpha\beta''}(R^{\alpha\beta^2}) G_{ij} G_{kl} R_i^{\alpha\beta} R_j^{\alpha\beta} R_k^{\alpha\beta} R_l^{\alpha\beta}. \end{aligned} \quad (21)$$

In an analogous manner one obtains:

$$\rho_\beta(r^{\alpha\beta^2}) = \rho_\beta(R^{\alpha\beta^2}) + 2\rho'_\beta(R^{\alpha\beta^2})G_{ij}R_j^{\alpha\beta}R_i^{\alpha\beta} + 2\rho''_\beta(R^{\alpha\beta^2})G_{ij}G_{kl}R_i^{\alpha\beta}R_j^{\alpha\beta}R_k^{\alpha\beta}R_l^{\alpha\beta}. \quad (22)$$

Here the abbreviations $(\diamond)'(R^{\alpha\beta^2})$ and $(\diamond)''(R^{\alpha\beta^2})$ represent the derivatives of (\diamond) with respect to its argument $r^{\alpha\beta^2}$ evaluated at $R^{\alpha\beta^2}$. Furthermore Eq (22) is of the form $\rho_\beta(r^{\alpha\beta^2}) = \mathcal{A}_\beta + \mathcal{B}_\beta\mathcal{X}_{\alpha\beta} + \frac{1}{2}\mathcal{C}_\beta\mathcal{X}_{\alpha\beta}^2$ with $\mathcal{A}_\beta = \rho_\beta(R^{\alpha\beta^2})$, $\mathcal{B}_\beta = \rho'_\beta(R^{\alpha\beta^2})$, $\mathcal{C}_\beta = \rho''_\beta(R^{\alpha\beta^2})$ and $\mathcal{X}_{\alpha\beta} = 2G_{ij}R_i^{\alpha\beta}R_j^{\alpha\beta}$. Consequently a Taylor expansion of $F_\alpha(\bar{\rho}_\alpha)$ at \mathcal{A}_β can be performed as follows:

$$\begin{aligned} F_\alpha\left(\sum_\beta \rho_\beta(r^{\alpha\beta^2})\right) &= F_\alpha\left(\sum_\beta \left[\mathcal{A}_\beta + \mathcal{B}_\beta\mathcal{X}_{\alpha\beta} + \frac{1}{2}\mathcal{C}_\beta\mathcal{X}_{\alpha\beta}^2\right]\right) = \\ &= F_\alpha\left(\sum_\beta \mathcal{A}_\beta\right) + \sum_\beta \left.\frac{\partial F_\alpha}{\partial \mathcal{X}_{\alpha\beta}}\right|_{\mathcal{X}_{\alpha\beta}=0} \mathcal{X}_{\alpha\beta} + \frac{1}{2} \sum_{\beta,\gamma} \left.\frac{\partial^2 F_\alpha}{\partial \mathcal{X}_{\alpha\beta} \partial \mathcal{X}_{\alpha\gamma}}\right|_{\mathcal{X}_{\alpha\beta}=\mathcal{X}_{\alpha\gamma}=0} \mathcal{X}_{\alpha\beta}\mathcal{X}_{\alpha\gamma}. \end{aligned} \quad (23)$$

Introducing:

$$A_{ij}^\alpha = \sum_\beta \phi^{\alpha\beta'}(R^{\alpha\beta^2})R_i^{\alpha\beta}R_j^{\alpha\beta}, \quad B_{ijkl}^\alpha = \sum_\beta \phi^{\alpha\beta''}(R^{\alpha\beta^2})R_i^{\alpha\beta}R_j^{\alpha\beta}R_k^{\alpha\beta}R_l^{\alpha\beta}, \quad (24)$$

$$V_{ij}^\alpha = \sum_\beta \rho'_\beta(R^{\alpha\beta^2})R_i^{\alpha\beta}R_j^{\alpha\beta}, \quad W_{ijkl}^\alpha = \sum_\beta \rho''_\beta(R^{\alpha\beta^2})R_i^{\alpha\beta}R_j^{\alpha\beta}R_k^{\alpha\beta}R_l^{\alpha\beta} \quad (25)$$

one can find the following important relation for the *energy of an arbitrary atom α* :

$$\begin{aligned} E_\alpha &= \frac{1}{2} \sum_\beta \phi^{\alpha\beta}(R^{\alpha\beta^2}) + F_\alpha(\bar{\rho}_\alpha^0) + G_{ij} \left[A_{ij}^\alpha + 2F'_\alpha(\bar{\rho}_\alpha^0)V_{ij}^\alpha \right] + \\ &\quad + G_{ij}G_{kl} \left[B_{ijkl}^\alpha + 2F'_\alpha(\bar{\rho}_\alpha^0)W_{ijkl}^\alpha + 2F''_\alpha(\bar{\rho}_\alpha^0)V_{ij}^\alpha V_{kl}^\alpha \right], \end{aligned} \quad (26)$$

where $F'_\alpha(\bar{\rho}_\alpha^0)$ and $F''_\alpha(\bar{\rho}_\alpha^0)$ refer the derivatives with respect to the argument at $\bar{\rho}_\alpha^0 = \sum_\beta \mathcal{A}_\beta = \sum_\beta \rho_\beta(R^{\alpha\beta^2})$. Note that in order to derive Eq (26) the chain rule was applied as follows:

$$\left.\frac{\partial F_\alpha}{\partial \mathcal{X}_{\alpha\beta}}\right|_{\mathcal{X}_{\alpha\beta}=0} = F'_\alpha\left(\sum_\beta \mathcal{A}_\beta\right) \cdot \sum_\beta \mathcal{B}_\beta, \quad (27)$$

$$\left.\frac{\partial^2 F_\alpha}{\partial \mathcal{X}_{\alpha\beta} \partial \mathcal{X}_{\alpha\gamma}}\right|_{\mathcal{X}_{\alpha\beta}=\mathcal{X}_{\alpha\gamma}=0} = F''_\alpha\left(\sum_\beta \mathcal{A}_\beta\right) \cdot \sum_{\beta,\gamma} \mathcal{B}_\beta\mathcal{B}_\gamma + F'_\alpha\left(\sum_\beta \mathcal{A}_\beta\right) \cdot \sum_\beta \mathcal{C}_\beta. \quad (28)$$

Eq (26) represents an important relation for the energy of atom α . It is valid in pure substances as well as in solid mixtures. In the case of solid mixtures one can find different types of atoms in the lattice, and we have to specify the type of α and of its neighbors β in more detail.

Moreover, neglecting thermal expansion, it is reasonable to postulate that E_α assumes a minimum at equilibrium. Thus in Eq (26) the first bracket on the right hand side must vanish and we find for the *equilibrium condition*:

$$A_{ij}^\alpha + 2F'_\alpha(\bar{\rho}_\alpha^0)V_{ij}^\alpha = 0. \quad (29)$$

Furthermore it holds $E_{\text{elast}}/V = \frac{1}{2}G_{ij}C_{ijkl}G_{kl}$ (law of Saint-Venant-Kirchhoff), [16]. Defining Ω_0^α as the volume occupied by an atom α we obtain for the *stiffness coefficients* from Eq (26):

$$C_{ijkl}^\alpha = \frac{1}{\Omega_0^\alpha} \left[2B_{ijkl}^\alpha + 4F'_\alpha(\bar{\rho}_\alpha^0)W_{ijkl}^\alpha + 4F''_\alpha(\bar{\rho}_\alpha^0)V_{ij}^\alpha V_{kl}^\alpha \right]. \quad (30)$$

At this point it should be pointed out that the underlying potentials of Eqns (29,30) depend on the argument $R^{\alpha\beta^2}$. Taking into account the chain rule and, in particular, the relations $\hat{\phi}^{\alpha\beta'}(R^{\alpha\beta^2}) = \frac{\phi^{\alpha\beta'}(R^{\alpha\beta})}{2R^{\alpha\beta}}$, $\hat{\rho}'_{\beta}(R^{\alpha\beta^2}) = \frac{\rho'_{\beta}(R^{\alpha\beta})}{2R^{\alpha\beta}}$, $\hat{\phi}^{\alpha\beta''}(R^{\alpha\beta^2}) = \frac{1}{4}(\frac{\phi^{\alpha\beta''}(R^{\alpha\beta})}{R^{\alpha\beta^2}} - \frac{\phi^{\alpha\beta'}(R^{\alpha\beta})}{R^{\alpha\beta^3}})$, and $\hat{\rho}''_{\beta}(R^{\alpha\beta^2}) = \frac{1}{4}(\frac{\rho''_{\beta}(R^{\alpha\beta})}{R^{\alpha\beta^2}} - \frac{\rho'_{\beta}(R^{\alpha\beta})}{R^{\alpha\beta^3}})$, Eqns (29,30) are in agreement with the accepted results communicated by Daw and Baskes in [13].

We already indicated the importance of Eqns (26,29,30) for solid mixtures. More specifically the question arises, how to specify these equations for different types of atoms. In the next section we want to turn the attention to binary alloys and present a procedure yielding all corresponding equations for binary mixtures.

4 EAM for binary alloys

4.1 Specification of the energy-expression: DPC operator and higher gradients

In context with Eq (26) the question arises, how to exploit this energy expression for binary alloys or, in other words, how additional information about the different types of atoms can be incorporated in this equation. In the case of a binary alloy A-B three different forms of interactions can be distinguished: A \leftrightarrow A, B \leftrightarrow B and A \leftrightarrow B interactions. In order to include these interaction terms in Eq (26) one can use a so called *Discrete Particle Concentration* (DPC) *operator*, introduced for example by de Fontaine, [17].

$$\hat{y}_{\gamma} = \begin{cases} 0, & \gamma = A \\ 1, & \gamma = B \end{cases} \quad (31)$$

We now have to detail the following expressions of Eq (26): $\phi^{\alpha\beta}$, $\bar{\rho}_{\alpha}^0$, F_{α} , A_{ij}^{α} , B_{ijkl}^{α} , $F'_{\alpha}V_{ij}^{\alpha}$, $F''_{\alpha}V_{ij}^{\alpha}V_{kl}^{\alpha}$ and $F'_{\alpha}W_{ijkl}^{\alpha}$. For this purpose we begin the analysis with the decomposition of $\phi^{\alpha\beta}$ and $\bar{\rho}_{\alpha}^0$ in the following manner:

$$\begin{aligned} \phi^{\alpha\beta} &= (1 - \hat{y}_{\alpha})(1 - \hat{y}_{\beta})\phi^{\text{AA}} + \hat{y}_{\alpha}\hat{y}_{\beta}\phi^{\text{BB}} + [(1 - \hat{y}_{\alpha})\hat{y}_{\beta} + (1 - \hat{y}_{\beta})\hat{y}_{\alpha}]\phi^{\text{AB}} \\ &= \phi^{\text{AA}} + [\hat{y}_{\alpha} + (1 - 2\hat{y}_{\alpha})\hat{y}_{\beta}]\phi + (\hat{y}_{\alpha} + \hat{y}_{\beta})\tilde{\phi}, \end{aligned} \quad (32)$$

$$\bar{\rho}_{\alpha}^0 = \sum_{\beta} [(1 - \hat{y}_{\beta})\rho_A + \hat{y}_{\beta}\rho_B] = \sum_{\beta} [\hat{y}_{\beta}(\rho_B - \rho_A) + \rho_A] \quad (33)$$

with the definitions $\phi = \phi^{\text{AB}} - \frac{1}{2}(\phi^{\text{AA}} + \phi^{\text{BB}})$ and $\tilde{\phi} = \frac{1}{2}(\phi^{\text{BB}} - \phi^{\text{AA}})$. Obviously the DCP operator act as a “selector” which “chooses” the corresponding interaction depending on what types of atoms are considered. If for example α and β are two A-atoms, \hat{y}_{α} as well as \hat{y}_{β} are zero and only the terms ϕ^{AA} and $\bar{\rho}_A^0 = \sum_{\beta} \rho_A$ remain in Eq (32) and (33). In a same manner one can obtain ϕ^{BB} , ϕ^{AB} and $\bar{\rho}_B^0$.

Moreover the DCP operator can be replaced by its continuous counterpart applying the mean

field limit. Thus a Taylor expansion results in:

$$\hat{y}_\alpha = y(X_i^\alpha) \equiv y(X_i), \quad (34)$$

$$\hat{y}_\beta = y(X_i^\beta) = y(X_i + R_i^{\alpha\beta}) = y(X_i) + \underbrace{\frac{\partial y}{\partial X_i} R_i^{\alpha\beta}}_{=\nabla_i y} + \frac{1}{2} \underbrace{\frac{\partial^2 y}{\partial X_i \partial X_j} R_i^{\alpha\beta} R_j^{\alpha\beta}}_{=\nabla_{ij}^2 y} + \dots \quad (35)$$

The symbols $\nabla_i y$ and $\nabla_{ij}^2 y$ are referred to as *higher gradients* and are characteristic of phase field theories. After a straightforward calculation we find:

$$\phi^{\alpha\beta} = \phi^{AA} + 2y(1-y)\phi + 2y\tilde{\phi} + \nabla_i y [(1-2y)\phi + \tilde{\phi}] R_i^{\alpha\beta} + \frac{1}{2} \nabla_{ij}^2 y [(1-2y)\phi + \tilde{\phi}] R_i^{\alpha\beta} R_j^{\alpha\beta}, \quad (36)$$

$$\bar{\rho}_\alpha^0 = \sum_\beta \rho_A + y \sum_\beta (\rho_B - \rho_A) + \nabla_i y \sum_\beta (\rho_B - \rho_A) R_i^{\alpha\beta} + \frac{1}{2} \nabla_{ij}^2 y \sum_\beta (\rho_B - \rho_A) R_i^{\alpha\beta} R_j^{\alpha\beta} \quad (37)$$

$$= \bar{\rho}^A + y\bar{\rho}^\Delta + (\nabla_i y)\bar{\rho}_i^\Delta + \frac{1}{2}(\nabla_{ij}^2 y)\bar{\rho}_{ij}^\Delta \quad (38)$$

with the definitions $\bar{\rho}^A = \sum_\beta \rho_A$; $\bar{\rho}^\Delta = \sum_\beta (\rho_B - \rho_A)$; $\bar{\rho}_i^\Delta = \sum_\beta (\rho_B - \rho_A) R_i^{\alpha\beta}$ and $\bar{\rho}_{ij}^\Delta = \sum_\beta (\rho_B - \rho_A) R_i^{\alpha\beta} R_j^{\alpha\beta}$. At this point it is important to mention that for any scalar function $f(R^{\alpha\beta})$ depending only on the *radial* distance $R^{\alpha\beta}$ between atom α and β the following sum vanishes:

$$\sum_\beta f(R^{\alpha\beta 2}) R_{i_1}^{\alpha\beta} \dots R_{i_N}^{\alpha\beta} = 0 \quad , \quad (\forall N = \text{odd number}). \quad (39)$$

This relation stems from the fact that in an arbitrary lattice, due to its periodic arrangement, for all vectors $R_i^{\alpha\beta}$ a vector $-R_i^{\alpha\beta}$ in opposite direction can be found (if boundary effects are neglected). Thus Eqns (36,38) results in:

$$\phi^{\alpha\beta} = \phi^{AA} + 2y(1-y)\phi + 2y\tilde{\phi} + \frac{1}{2} \nabla_{ij}^2 y [(1-2y)\phi + \tilde{\phi}] R_i^{\alpha\beta} R_j^{\alpha\beta}, \quad (40)$$

$$\bar{\rho}_\alpha^0 = \bar{\rho}^A + y\bar{\rho}^\Delta + \frac{1}{2}(\nabla_{ij}^2 y)\bar{\rho}_{ij}^\Delta. \quad (41)$$

Using Eq (38) the embedding function $F_\alpha(\bar{\rho}_\alpha^0)$ can be also expanded into a Taylor series evaluated at a *weighted average electron density* $\bar{\rho}_{av} = \bar{\rho}^A + y\bar{\rho}^\Delta = (1-y)\bar{\rho}_A + y\bar{\rho}_B$:

$$F_\alpha(\bar{\rho}_\alpha^0) = F_\alpha\left(\underbrace{\bar{\rho}^A + y\bar{\rho}^\Delta}_{=\bar{\rho}_{av}} + \frac{1}{2}(\nabla_{ij}^2 y)\bar{\rho}_{ij}^\Delta\right) = F_\alpha(\bar{\rho}_{av}) + \frac{1}{2}F'_\alpha(\bar{\rho}_{av}) \bar{\rho}_{ij}^\Delta (\nabla_{ij}^2 y) + \dots \quad (42)$$

Note that gradient terms of higher than second order were assumed not to contribute to the energy of the system. Moreover, F_α itself is also decomposed analogously to Eq (33) and we write:

$$F_\alpha(\bar{\rho}_\alpha^0) = (1-y)F_A + yF_B, \quad (43)$$

$$F_A = F_A(\bar{\rho}_{av}) + \frac{1}{2}F'_A(\bar{\rho}_{av})\bar{\rho}_{ij}^\Delta(\nabla_{ij}^2 y) \dots \quad , \quad F_B = F_B(\bar{\rho}_{av}) + \frac{1}{2}F'_B(\bar{\rho}_{av})\bar{\rho}_{ij}^\Delta(\nabla_{ij}^2 y) \dots \quad (44)$$

So the first two terms of the right hand side of Eq (26) are specified in terms of concentration gradients by Eqns (36) and (43-44).

In what follows we want to investigate the symbols A_{ij}^α , B_{ijkl}^α , $F_\alpha' V_{ij}^\alpha$, $F_\alpha'' V_{ij}^\alpha V_{kl}^\alpha$ and $F_\alpha' W_{ijkl}^\alpha$ of Eq (26). Here it is worth mentioning that the products of the last three expressions $F_\alpha' V_{ij}^\alpha$, $F_\alpha'' V_{ij}^\alpha V_{kl}^\alpha$ and $F_\alpha' W_{ijkl}^\alpha$ cannot be separated and evaluated separately since *they are coupled by the same index α* . Hence the decomposition by means of the DCP-operator must be applied to the complete product.

The first two abbreviations, A_{ij}^α and B_{ijkl}^α , can be written in the same manner as in Eq (36):

$$A_{ij}^\alpha = A_{ij}^\Lambda + 2y(1-y)A_{ij}^\phi + 2yA_{ij}^{\tilde{\phi}} + \frac{1}{2}\nabla_{kl}^2 y \left[(1-2y)A_{ijkl}^\phi + A_{ijkl}^{\tilde{\phi}} \right], \quad (45)$$

$$B_{ijkl}^\alpha = B_{ijkl}^\Lambda + 2y(1-y)B_{ijkl}^\phi + 2yB_{ijkl}^{\tilde{\phi}} + \frac{1}{2}\nabla_{mn}^2 y \left[(1-2y)B_{ijklmn}^\phi + B_{ijklmn}^{\tilde{\phi}} \right] \quad (46)$$

with the definitions:

$$A_{ij}^\Lambda = \sum_{\beta} \phi^{\Lambda\Lambda'}(R^{\alpha\beta^2}) R_i^{\alpha\beta} R_j^{\alpha\beta} \quad , \quad A_{ijkl}^\phi = \sum_{\beta} \phi'(R^{\alpha\beta^2}) R_i^{\alpha\beta} R_j^{\alpha\beta} R_k^{\alpha\beta} R_l^{\alpha\beta} \quad , \quad (47)$$

$$A_{ijkl}^{\tilde{\phi}} = \sum_{\beta} \tilde{\phi}'(R^{\alpha\beta^2}) R_i^{\alpha\beta} R_j^{\alpha\beta} R_k^{\alpha\beta} R_l^{\alpha\beta} \quad , \quad B_{ijkl}^\Lambda = \sum_{\beta} \phi^{\Lambda\Lambda''}(R^{\alpha\beta^2}) R_i^{\alpha\beta} R_j^{\alpha\beta} R_k^{\alpha\beta} R_l^{\alpha\beta} \quad (48)$$

$$B_{ijklmn}^\phi = \sum_{\beta} \phi''(R^{\alpha\beta^2}) R_i^{\alpha\beta} \dots R_n^{\alpha\beta} \quad , \quad B_{ijklmn}^{\tilde{\phi}} = \sum_{\beta} \tilde{\phi}''(R^{\alpha\beta^2}) R_i^{\alpha\beta} \dots R_n^{\alpha\beta} \quad . \quad (49)$$

Analogously to Eq (43) the following relations hold:

$$F_\alpha'(\bar{\rho}_\alpha^0) V_{ij}^\alpha = (1-y)F_A' V_{ij}^\alpha \Big|_{\alpha=A} + yF_B' V_{ij}^\alpha \Big|_{\alpha=B}, \quad (50)$$

$$F_\alpha'(\bar{\rho}_\alpha^0) W_{ijkl}^\alpha = (1-y)F_A' W_{ijkl}^\alpha \Big|_{\alpha=A} + yF_B' W_{ijkl}^\alpha \Big|_{\alpha=B}, \quad (51)$$

$$F_\alpha''(\bar{\rho}_\alpha^0) V_{ij}^\alpha V_{kl}^\alpha = (1-y)F_A'' V_{ij}^\alpha V_{kl}^\alpha \Big|_{\alpha=A} + yF_B'' V_{ij}^\alpha V_{kl}^\alpha \Big|_{\alpha=B}. \quad (52)$$

The derivatives F_α' and F_α'' can be calculated analogously to Eqns (44). We simply increase the order of derivatives in these equations:

$$F_{A/B}' = F_{A/B}'(\bar{\rho}_{av}) + \frac{1}{2}F_{A/B}''(\bar{\rho}_{av})\bar{\rho}_{ij}^\Delta(\nabla_{ij}^2 y), \quad (53)$$

$$F_{A/B}'' = F_{A/B}''(\bar{\rho}_{av}) + \frac{1}{2}F_{A/B}'''(\bar{\rho}_{av})\bar{\rho}_{ij}^\Delta(\nabla_{ij}^2 y). \quad (54)$$

By combination of Eqns (25) and (41) we finally find ($\alpha = \{A,B\}$):

$$V_{ij}^\alpha = V_{ij}^\Lambda + yV_{ij}^\Delta + \frac{1}{2}(\nabla_{kl}^2 y)V_{ijkl}^\Delta, \quad (55)$$

$$W_{ijkl}^\alpha = W_{ijkl}^\Lambda + yW_{ijkl}^\Delta + \frac{1}{2}(\nabla_{mn}^2 y)W_{ijklmn}^\Delta \quad (56)$$

with the abbreviations:

$$V_{ij}^\Lambda = \sum_{\beta} \rho_A'(R^{\alpha\beta^2}) R_i^{\alpha\beta} R_j^{\alpha\beta} \quad , \quad V_{i_1, \dots, i_n}^\Delta = \sum_{\beta} \left[\rho_B'(R^{\alpha\beta^2}) - \rho_A'(R^{\alpha\beta^2}) \right] R_{i_1}^{\alpha\beta} \dots R_{i_n}^{\alpha\beta}, \quad (57)$$

$$W_{ijkl}^\Lambda = \sum_{\beta} \rho_A''(R^{\alpha\beta^2}) R_i^{\alpha\beta} \dots R_l^{\alpha\beta} \quad , \quad W_{i_1, \dots, i_n}^\Delta = \sum_{\beta} \left[\rho_B''(R^{\alpha\beta^2}) - \rho_A''(R^{\alpha\beta^2}) \right] R_{i_1}^{\alpha\beta} \dots R_{i_n}^{\alpha\beta} \quad (58)$$

and all terms of Eq (26) are now specified for a binary alloy A-B. In the following section it is shown how these cumbersome equations can be structured in order to obtain information regarding the equilibrium condition, the stiffness and the higher gradient coefficients.

4.2 Equilibrium condition, stiffness and higher gradient coefficients

By combination of Eq (26) with Eqns (40, 43, 44, 45, 46, 50-56) and by means of the definitions:

$$g^{\text{AA}} = \sum_{\beta} \phi^{\text{AA}} \quad , \quad g^{\phi} = \sum_{\beta} \phi \quad , \quad g^{\tilde{\phi}} = \sum_{\beta} \tilde{\phi} \quad , \quad (59)$$

$$g_{ij}^{\phi} = \sum_{\beta} \phi R_i^{\alpha\beta} R_j^{\alpha\beta} \quad , \quad g_{ij}^{\tilde{\phi}} = \sum_{\beta} \tilde{\phi} R_i^{\alpha\beta} R_j^{\alpha\beta} . \quad (60)$$

we obtain for the energy of atom α :

$$\begin{aligned} E_{\alpha} = & \frac{1}{2}g^{\text{AA}} + y(1-y)g^{\phi} + yg^{\tilde{\phi}} + \frac{1}{4}(\nabla_{ij}^2 y) \left[(1-2y)g_{ij}^{\phi} + g_{ij}^{\tilde{\phi}} \right] + \\ & + F_{\text{A}} + y(F_{\text{B}} - F_{\text{A}}) + \frac{1}{2}(\nabla_{ij}^2 y) \bar{\rho}_{ij}^{\Delta} \left[F'_{\text{A}} + y(F'_{\text{B}} - F'_{\text{A}}) \right] + \\ & + G_{ij} \left\{ A_{ij}^{\text{A}} + 2y(1-y)A_{ij}^{\phi} + 2yA_{ij}^{\tilde{\phi}} + \frac{1}{2}(\nabla_{kl}^2 y) \left[(1-2y)A_{ijkl}^{\phi} + A_{ijkl}^{\tilde{\phi}} \right] + \right. \\ & + 2(V_{ij}^{\text{A}} + yV_{ij}^{\Delta}) \left(F'_{\text{A}} + y(F'_{\text{B}} - F'_{\text{A}}) \right) + \\ & \left. + (\nabla_{kl}^2 y) \left[V_{ijkl}^{\Delta} \left(F'_{\text{A}} + y(F'_{\text{B}} - F'_{\text{A}}) \right) + \bar{\rho}_{kl}^{\Delta} \left(V_{ij}^{\text{A}} + yV_{ij}^{\Delta} \right) \left(F''_{\text{A}} + y(F''_{\text{B}} - F''_{\text{A}}) \right) \right] \right\} + \\ & + \frac{1}{2}G_{ij}G_{kl} \left\{ 2B_{ijkl}^{\text{A}} + 4y(1-y)B_{ijkl}^{\phi} + 4yB_{ijkl}^{\tilde{\phi}} + (\nabla_{mn}^2 y) \left[(1-2y)B_{ijklmn}^{\phi} + B_{ijklmn}^{\tilde{\phi}} \right] + \right. \\ & + 4(W_{ijkl}^{\text{A}} + yW_{ijkl}^{\Delta}) \left(F'_{\text{A}} + y(F'_{\text{B}} - F'_{\text{A}}) \right) + \\ & + 2(\nabla_{mn}^2 y) \left[W_{ijklmn}^{\Delta} \left(F'_{\text{A}} + y(F'_{\text{B}} - F'_{\text{A}}) \right) + \bar{\rho}_{mn}^{\Delta} \left(W_{ijkl}^{\text{A}} + yW_{ijkl}^{\Delta} \right) \left(F''_{\text{A}} + y(F''_{\text{B}} - F''_{\text{A}}) \right) \right] + \\ & + 4(V_{ij}^{\text{A}} + yV_{ij}^{\Delta}) \left(V_{kl}^{\text{A}} + yV_{kl}^{\Delta} \right) \left(F''_{\text{A}} + y(F''_{\text{B}} - F''_{\text{A}}) \right) + \\ & + 2(\nabla_{mn}^2 y) \left[V_{klmn}^{\Delta} \left(V_{ij}^{\text{A}} + yV_{ij}^{\Delta} \right) \left(F''_{\text{A}} + y(F''_{\text{B}} - F''_{\text{A}}) \right) + V_{ijmn}^{\Delta} \left(V_{kl}^{\text{A}} + yV_{kl}^{\Delta} \right) \times \right. \\ & \left. \left. \times \left(F''_{\text{A}} + y(F''_{\text{B}} - F''_{\text{A}}) \right) + \bar{\rho}_{mn}^{\Delta} \left(V_{ij}^{\text{A}} + yV_{ij}^{\Delta} \right) \left(V_{kl}^{\text{A}} + yV_{kl}^{\Delta} \right) \left(F'''_{\text{A}} + y(F'''_{\text{B}} - F'''_{\text{A}}) \right) \right] \right\} \quad (61) \end{aligned}$$

where $F_{\text{A/B}}$ and all derivatives of $F_{\text{A/B}}$ depend on the argument $\bar{\rho}_{av}$!!!

Following Cahn and Hilliard in [6] and Dreyer and Müller in [2, 11] the Gibbs free energy density ψ of a two-component system with an *inhomogeneous* mass-concentration profile $c(x_i, t)$ can be characterized by the equation (without eigenstrains and thermal expansion):

$$\psi = \psi_{\text{conf}}(c, G_{ij}) - a_{kl}(c, G_{ij}) \nabla_{kl}^2 c + b_{kl}(c, G_{ij}) (\nabla_k c) (\nabla_l c) . \quad (62)$$

The first term denotes the configurational part of ψ and represents the Gibbs free energy density of the corresponding system with a *homogeneous* concentration profile. It also includes an “elastic” energy, ψ_{elast} , as reflected by the strains G_{kl} . Therefore one can split ψ_{conf} into two

parts:

$$\psi_{\text{conf}}(c, G_{ij}) = \psi_0(c) + \underbrace{\frac{1}{2} G_{ij} C_{ijkl}(c) G_{kl}}_{=\psi_{\text{elast}}}, \quad (63)$$

where the first part stands for the energy density *without* elastic energy contributions. Moreover it is important to mention that ψ_{elast} does not contain higher gradients and, consequently, it is reasonable to re-arrange Eq (61) as follows:

$$\begin{aligned} E_\alpha &= \frac{1}{2} g^{\text{AA}} + y(1-y)g^\phi + yg^{\tilde{\phi}} + F_A + y(F_B - F_A) \\ &+ \frac{1}{2} G_{ij} G_{kl} \left\{ 2B_{ijkl}^{\text{A}} + 4y(1-y)B_{ijkl}^\phi + 4yB_{ijkl}^{\tilde{\phi}} + 4(W_{ijkl}^{\text{A}} + yW_{ijkl}^\Delta)(F'_A + y(F'_B - F'_A)) \right. \\ &\quad \left. + 4(V_{ij}^{\text{A}} + yV_{ij}^\Delta)(V_{kl}^{\text{A}} + yV_{kl}^\Delta)(F''_A + y(F''_B - F''_A)) \right\} \\ &+ (\nabla_{mn}^2 y) \left\{ \frac{1}{4} \left((1-2y)g_{mn}^\phi + g_{mn}^{\tilde{\phi}} \right) + \frac{1}{2} \bar{\rho}_{mn}^\Delta (F'_A + y(F'_B - F'_A)) \right. \\ &\quad + \frac{1}{2} G_{ij} \left[(1-2y)A_{ijmn}^\phi + A_{ijmn}^{\tilde{\phi}} + 2V_{ijmn}^\Delta (F'_A + y(F'_B - F'_A)) \right. \\ &\quad \left. + 2\bar{\rho}_{mn}^\Delta (V_{ij}^{\text{A}} + yV_{ij}^\Delta)(F''_A + y(F''_B - F''_A)) \right] \\ &\quad + \frac{1}{2} G_{ij} G_{kl} \left[(1-2y)B_{ijklmn}^\phi + B_{ijklmn}^{\tilde{\phi}} \right. \\ &\quad + 2W_{ijklmn}^\Delta (F'_A + y(F'_B - F'_A)) + 2\bar{\rho}_{mn}^\Delta (W_{ijkl}^{\text{A}} + yW_{ijkl}^\Delta)(F''_A + y(F''_B - F''_A)) \\ &\quad + 2V_{klmn}^\Delta (V_{ij}^{\text{A}} + yV_{ij}^\Delta)(F''_A + y(F''_B - F''_A)) + 2V_{ijmn}^\Delta (V_{kl}^{\text{A}} + yV_{kl}^\Delta) \times \\ &\quad \left. \left. \times (F''_A + y(F''_B - F''_A)) + 2\bar{\rho}_{mn}^\Delta (V_{ij}^{\text{A}} + yV_{ij}^\Delta)(V_{kl}^{\text{A}} + yV_{kl}^\Delta)(F'''_A + y(F'''_B - F'''_A)) \right] \right\} \\ &+ G_{ij} \left\{ A_{ij}^{\text{A}} + 2y(1-y)A_{ij}^\phi + 2yA_{ij}^{\tilde{\phi}} + 2(V_{ij}^{\text{A}} + yV_{ij}^\Delta)(F'_A + y(F'_B - F'_A)) \right\}. \quad (64) \end{aligned}$$

Equation (64) consists of four parts (1st row; 2nd and 3rd row; 4th-10th row; last row).

- The first part represents the energy of an atom α in an undeformed, homogeneous (i.e., without concentration gradients) solid, according to ψ_0 in Eq (63).
- The second part denotes the elastic energy ψ_{elast} of a mixture with *particle* concentration y .
- The third part can be related to the HGCs. Note that in Eq (64) only derivatives $\nabla_{kl}^2 y$ occur. A substitution to $\nabla_{kl}^2 c$ will later allow the identification of a_{kl} and b_{kl} of Eq (62).
- The last part stands for the equilibrium condition of a binary mixture A-B (minimum of energy), namely $\partial E_\alpha / \partial G_{ij} |_{G_{ij}=0, y=y^{\text{eq}}} = 0 \Rightarrow A_{ij}^{\text{A}} + 2y(1-y)A_{ij}^\phi + 2yA_{ij}^{\tilde{\phi}} + 2(V_{ij}^{\text{A}} + yV_{ij}^\Delta)(F'_A +$

$y(F'_B - F'_A) = 0$. By knowing the equilibrium concentration y^{eq} this condition can be used to obtain the equilibrium nearest neighbor distance R in the different equilibrium phases.

At this point it should be mentioned that all atomistic considerations are performed with respect to the particle concentration y . In order to identify the quantities in Eq (2) we have to switch to mass concentrations c . Following the arguments of Appendix B we finally find:

◇ *equilibrium condition:*

$$A_{ij}^A + 2y(c)(1 - y(c))A_{ij}^\phi + 2y(c)A_{ij}^{\tilde{\phi}} + 2\left(V_{ij}^A + y(c)V_{ij}^\Delta\right)\left(F'_A + y(c)(F'_B - F'_A)\right) = 0 \quad (65)$$

◇ *Stiffness coefficients:*

$$C_{ijkl}(c) = \frac{1}{\Omega_0^\alpha} \left[2B_{ijkl}^A + 4y(c)(1 - y(c))B_{ijkl}^\phi + 4y(c)B_{ijkl}^{\tilde{\phi}} + 4\left(W_{ijkl}^A + y(c)W_{ijkl}^\Delta\right) \times \right. \\ \left. \times \left(F'_A + y(c)(F'_B - F'_A)\right) + 4\left(V_{ij}^A + y(c)V_{ij}^\Delta\right)\left(V_{kl}^A + y(c)V_{kl}^\Delta\right)\left(F''_A + y(c)(F''_B - F''_A)\right) \right] \quad (66)$$

◇ *Higher gradient coefficients:*

$$a_{mn}(c, G_{pq}) = -\delta(c) M^{(2)}(c) \mathbb{H}_{mn}(c, G_{pq}), \quad (67)$$

$$b_{mn}(c, G_{pq}) = \delta(c) M^{(1)}(c) \mathbb{H}_{mn}(c, G_{pq}), \quad (68)$$

$$A_{mn}(c, G_{pq}) = \frac{\partial a_{mn}(c, G_{pq})}{\partial c} + b_{mn}(c, G_{pq}) \quad (69)$$

with

$$\delta(c) = \frac{\rho_0}{\mu_0 M(c)}, \quad M^{(1)}(c) = \frac{2M_A M_B (M_B - M_A)}{[M_B - (M_B - M_A)c]^3}, \quad M^{(2)}(c) = \frac{M_A M_B}{[M_B - (M_B - M_A)c]^2}, \quad (70)$$

$$\mathbb{H}_{mn}(c, G_{pq}) = \frac{1}{4} \left((1 - 2y(c))g_{mn}^\phi + g_{mn}^{\tilde{\phi}} \right) + \frac{1}{2}\bar{\rho}_{mn}^\Delta \left(F'_A + y(c)(F'_B - F'_A) \right) \\ + \frac{1}{2}G_{ij} \left[(1 - 2y(c))A_{ijmn}^\phi + A_{ijmn}^{\tilde{\phi}} + 2V_{ijmn}^\Delta \left(F'_A + y(c)(F'_B - F'_A) \right) \right. \\ \left. + 2\bar{\rho}_{mn}^\Delta \left(V_{ij}^A + y(c)V_{ij}^\Delta \right) \left(F''_A + y(c)(F''_B - F''_A) \right) \right] \\ + \frac{1}{2}G_{ij}G_{kl} \left[(1 - 2y(c))B_{ijklmn}^\phi + B_{ijklmn}^{\tilde{\phi}} \right. \\ + 2W_{ijklmn}^\Delta \left(F'_A + y(c)(F'_B - F'_A) \right) + 2\bar{\rho}_{mn}^\Delta \left(W_{ijkl}^A + y(c)W_{ijkl}^\Delta \right) \left(F''_A + y(c)(F''_B - F''_A) \right) \\ + 2V_{klmn}^\Delta \left(V_{ij}^A + y(c)V_{ij}^\Delta \right) \left(F''_A + y(c)(F''_B - F''_A) \right) + 2V_{ijmn}^\Delta \left(V_{kl}^A + y(c)V_{kl}^\Delta \right) \times \\ \left. \times \left(F''_A + y(c)(F''_B - F''_A) \right) + 2\bar{\rho}_{mn}^\Delta \left(V_{ij}^A + y(c)V_{ij}^\Delta \right) \left(V_{kl}^A + y(c)V_{kl}^\Delta \right) \left(F'''_A + y(c)(F'''_B - F'''_A) \right) \right]. \quad (71)$$

Recall that all atomistic quantities refer to arguments $R^{\alpha\beta^2}$ and $\bar{\rho}_{av}$, respectively. In the following section we consider a specific binary alloy and will explicitly determine the stiffness and the higher gradient coefficients.

5 Application to the Ag-Cu system

As a case study we choose $y \equiv y_{\text{Cu}}$ ($c \equiv c_{\text{Cu}}$) and consider the solid eutectic binary alloy Ag-Cu at 1000 Kelvin ($y_{\text{eut}} = 0.41$, $c_{\text{eut}} = 0.29$, $T_{\text{eut}} \approx 1052$ Kelvin) which, from a technological point of view, serves as a brazing material. Two different equilibrium phases are observed, the α - and the β -phase, with the equilibrium concentrations c_α and c_β , respectively (cf., Fig. 1). Fig. 5 shows the specific Gibbs free curve, $\psi(c)$, at 1000 Kelvin. It was obtained from a commercial database, [18]. By means of the common tangent rule construction the following equilibrium concentrations $c^{\alpha/\beta}$ were determined:

$$c^\alpha = 0.063 \quad \Leftrightarrow \quad y^\alpha = 0.102, \quad (72)$$

$$c^\beta = 0.945 \quad \Leftrightarrow \quad y^\beta = 0.967. \quad (73)$$

Moreover both species Ag and Cu as well as the alloy Ag-Cu form a simple Face-Centered-Cubic (FCC) lattice so that this material is particularly suited for our atomistic investigations performed at the two equilibrium concentrations, $c^{\alpha/\beta}$. Before we turn to the fitting procedure some remarks, assumptions, and interpretations in context with Eq (64) will be made which are required for further investigations.

1. E_α stands for the energy of an atom α in a binary lattice, where two types of atoms (A and B) and three types of interactions (A-A, B-B, A-B) are possible.
2. Independent of these different interactions and atom-types it is assumed that only *one* equilibrium distance R to the nearest neighbors can be found in the lattice³.
3. All quantities of the right hand side of Eq (64): $g^{\text{AA}/\phi/\tilde{\phi}}$, $B_{ijkl}^{\text{A}/\phi/\tilde{\phi}}$, $F_{\text{A/B}}$, $F'_{\text{A/B}}$, $F''_{\text{A/B}}$, $F'''_{\text{A/B}}$, $V_{ij}^{\text{A}/\Delta}$, $W_{ijkl}^{\text{A}/\Delta}$, etc., can be calculated from the pure substances A and B. The ‘‘combination’’ of these quantities according to Eq (64) in terms of y , $(1-y)$, $\nabla_{mn}^2 y$, etc. is interpreted as a suitable average describing the energy of an arbitrary particle in the mixture A-B.

The second bullet point gives rise to the question of how to find the equilibrium nearest neighbor distance of a given phase (mixture) with the equilibrium concentration c^{eq} . In this context we can revert to the equilibrium condition given by Eq (65), provided that c^{eq} is known (e.g., from experiments).

For the sake of transparency we will now give an overview of the further procedures required to obtain the different EAM potentials, the stiffness and the higher gradient coefficients. **(1)** The EAM potentials for the pure substances Ag and Cu are fitted in terms of $R^{\alpha\beta^2}$. **(2)** We calculate the stiffness coefficients for the pure substances and compare them with experimental results (for the purpose of checking). **(3)** An exploitation of the equilibrium condition is performed in order to determine the nearest neighbor distances of the α - and β -phase in Ag-Cu at 1000 K. **(4)** The stiffness coefficients of the different phases $C_{ijkl}^{\alpha/\beta}$ are determined and the pure-substance-limit (i.e., Ag: $\lim c^{\alpha/\beta} = 0$

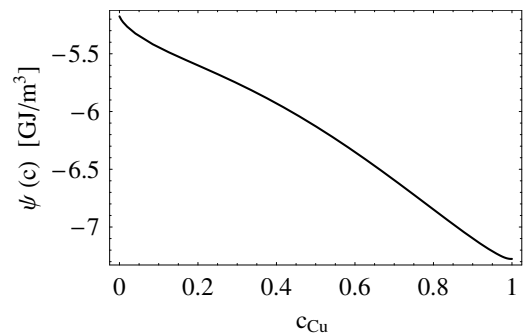


Figure 5: The Gibbs free energy density $\psi(c)$ for the Ag-Cu system at 1000 Kelvin.

³This assumption can be interpreted as an ‘‘effective’’ lattice, owing the same total cohesive energy as an lattice, where three different nearest neighbor distances occur, depending on the three different interactions.

and Cu: $\lim c^{\alpha/\beta} = 1$) is performed. **(5)** The HGCs in the α - and β -phases are calculated for the strain-free case (for convenience). **(6)** The phase-diagram of Ag-Cu is constructed and the results are compared with measurements in order to emphasize the “quality” of the predicted HGCs.

5.1 The fitting procedure for Ag and Cu

Recall the advantages of the use of potentials in terms of $r^{\alpha\beta^2}$ or $R^{\alpha\beta^2}$, respectively as outlined in Subsection 3.1. For this reason we modify Johnson’s functional representation from Eq (5) as follows:

$$\rho(r^2) = \rho_e \exp \left[-\beta \left(\frac{r^2}{R^2} - 1 \right) \right] \quad , \quad \phi(r^2) = \phi_e \exp \left[-\gamma \left(\frac{r^2}{R^2} - 1 \right) \right]. \quad (74)$$

The symbols r and R denote the nearest neighbor distance in the deformed and in the undeformed lattice and, in an FCC ensemble, are given by $a\sqrt{2}$ or $a_e\sqrt{2}$ (cf., Fig 3). Moreover the following relations hold:

$$\bar{\rho}(r^2) = 12\rho(r^2) \quad , \quad \bar{\rho}_e = 12\rho_e \quad , \quad \frac{1}{2} \sum_{\beta} \phi(r^2) = 6\phi(r^2) \quad , \quad 6\phi_e \equiv \Phi_e. \quad (75)$$

In order to arrive at an explicit relation for the embedding function $F(\bar{\rho})$ analogously to Eq (10) we follow the strategy explained in Section 2.2 and use the following inversions:

$$\frac{r}{R} = \sqrt{1 - \frac{1}{\beta} \ln \frac{\bar{\rho}}{\bar{\rho}_e}} \quad , \quad \frac{\phi}{\phi_e} = \left(\frac{\bar{\rho}}{\bar{\rho}_e} \right)^{\frac{\gamma}{\beta}}. \quad (76)$$

By means of the universal function of state $E(a)$ from Section 2.2 and Eq (76) the following result is obtained:

$$F(\bar{\rho}) = -E_{\text{sub}} \left[1 + \alpha \left(\sqrt{1 - \frac{1}{\beta} \ln \frac{\bar{\rho}}{\bar{\rho}_e}} - 1 \right) \right] \exp \left[-\alpha \left(\sqrt{1 - \frac{1}{\beta} \ln \frac{\bar{\rho}}{\bar{\rho}_e}} - 1 \right) \right] - \Phi_e \left(\frac{\bar{\rho}}{\bar{\rho}_e} \right)^{\frac{\gamma}{\beta}}. \quad (77)$$

with $\alpha = 3\sqrt{\frac{\kappa\Omega_0}{E_{\text{sub}}}}$.

In what follows we focus on the pure substances Ag and Cu as well as on the binary alloy Ag-Cu (silver-copper). In the case of the pure materials the following functions must be determined: ϕ^{AgAg} , ϕ^{CuCu} , ρ_{Ag} ($= 1/12\bar{\rho}_{\text{Ag}}$), ρ_{Cu} ($= 1/12\bar{\rho}_{\text{Cu}}$), $F_{\text{Ag}}(\bar{\rho}_{\text{Ag}})$, and $F_{\text{Cu}}(\bar{\rho}_{\text{Cu}})$. Thus for *both* pure components five parameters must be fitted, namely α , β , γ , ϕ_e , ρ_e . Consequently ten parameters are unknown. Note that the interaction between an Ag and a Cu nucleus, i.e., ϕ^{AgCu} , follows directly from considering the pure species Ag and Cu (cf., Eq (6)). For the fitting procedure the following ten experimental parameters of both substances are used:

1. VOIGT average of the shear modulus G
2. compressibility κ
3. sublimation energy E_{sub} (with respect to one particle)
4. (unrelaxed) vacancy formation energy E_{uvf}
5. (equilibrium) lattice parameter a_e

α is already given by Eq (10)₂, i.e., it only remains to determine β , γ , ϕ_e , and ρ_e .

Determination of ϕ_e and ρ_e Following Johnson in [19] the sublimation energy per atom (i.e., the cohesive energy) of an arbitrary atom is represented by the nuclei-nuclei interactions with its neighbors: $E_{\text{sub}} = \frac{1}{2} \cdot 12 \cdot \phi(r^2)$. Hence it follows for equilibrium:

$$\phi_e = \frac{E_{\text{sub}}}{6}. \quad (78)$$

From the physical point of view it is plausible to establish that $\rho_e \propto 1/\Omega_0$ and $\rho_e \propto E_{\text{sub}}$ and, consequently, we write:

$$\rho_e = \frac{E_{\text{sub}}}{\Omega_0}. \quad (79)$$

The last two equations represent two relations for the unknown material parameters ϕ_e and ρ_e .

Determination of β and γ The starting point to obtain these quantities are the equations for the unrelaxed vacancy formation energy E_{uvf} and the VOIGT average of the shear modulus G :

$$E_{\text{uvf}} = -\frac{1}{2} \sum_{\beta=1}^{12} \phi(r^2) - \sum_{\beta=1}^{12} F[12\rho(r^2)] + \sum_{\beta=1}^{12} F[11\rho(r^2)], \quad (80)$$

$$G = \frac{1}{5}(3C_{2323} + 2C^*) \quad , \quad C^* = \frac{1}{2}(C_{1111} - C_{1122}) \quad (81)$$

where C_{1111} , C_{1122} , and C_{2323} denote the elastic constants of the fourth order stiffness matrix. These constants are characterized by derivatives of the energy expression of a solid (Eq. (4)). Recall that for the stiffness C_{ijkl} of a pure substance A (cf., Eq (30)) we have:

$$C_{ijkl}^A = \frac{1}{\Omega_0^A} \left[2B_{ijkl}^{AA} + 4F'_A(\bar{\rho}_A^0) W_{ijkl}^A + 4F''_A(\bar{\rho}_A^0) V_{ij}^A V_{kl}^A \right] \quad (30a)$$

with the definitions:

$$\bar{\rho}_A^0 = \sum_{\beta} \rho_A(R^{\alpha\beta^2}) \quad , \quad B_{ijkl}^{AA} = \sum_{\beta} \phi^{AA''}(R^{\alpha\beta^2}) R_i^{\alpha\beta} R_j^{\alpha\beta} R_k^{\alpha\beta} R_l^{\alpha\beta} \quad , \quad (82)$$

$$V_{ij}^A = \sum_{\beta} \rho'_A(R^{\alpha\beta^2}) R_i^{\alpha\beta} R_j^{\alpha\beta} \quad , \quad W_{ijkl}^A = \sum_{\beta} \rho''_A(R^{\alpha\beta^2}) R_i^{\alpha\beta} R_j^{\alpha\beta} R_k^{\alpha\beta} R_l^{\alpha\beta} \quad , \quad (83)$$

$$F'_A = \left. \frac{\partial F_A}{\partial \bar{\rho}_A} \right|_{\bar{\rho}_A = \bar{\rho}_A^0} \quad , \quad F''_A = \left. \frac{\partial^2 F_A}{\partial \bar{\rho}_A^2} \right|_{\bar{\rho}_A = \bar{\rho}_A^0} \quad , \quad \phi^{AA''} = \left. \frac{\partial^2 \phi^{AA}}{\partial (r^{\alpha\beta^2})^2} \right|_{r^{\alpha\beta^2} = R^{\alpha\beta^2}} \quad , \quad (84)$$

$$\rho'_A = \left. \frac{\partial \rho_A}{\partial r^{\alpha\beta^2}} \right|_{r^{\alpha\beta^2} = R^{\alpha\beta^2}} \quad , \quad \rho''_A = \left. \frac{\partial^2 \rho_A}{\partial (r^{\alpha\beta^2})^2} \right|_{r^{\alpha\beta^2} = R^{\alpha\beta^2}} \quad , \quad (85)$$

where $r^{\alpha\beta^2}$ or $R^{\alpha\beta^2}$ represent the distance between the atoms α and β and can be identified with r^2 or R^2 in the nearest neighbor model.

Relation (30a) for the elastic constants can be used in Eq (81)_{1,2}. Then together with the parameterizations (74,75,77) it follows that (cf., Appendix C):

$$G = \frac{8}{5} \frac{\gamma(\gamma - \beta)}{\Omega_0}. \quad (86)$$

In a similar manner it is possible to *approximate* the unrelaxed vacancy formation energy E_{uvf} in Eq (80) by (cf., Appendix C):

$$E_{\text{uvf}} \approx \frac{15 G \Omega_0}{4 \gamma \beta} = 6 \phi_e \frac{\gamma - \beta}{\beta}. \quad (87)$$

The last two relations represent two equations for β and γ . As input we use the VOIGT average of the shear modulus and the unrelaxed vacancy formation energy. Using now Eqs (10)₂, (78), (79), (86), and (87), we can determine all parameters for Ag and Cu. The experimental data required during this procedure are compiled in Table 1, [19]:

Table 1: Experimental data for Ag and Cu

type of atom	Input				
	Ω_0 in \AA^3	E_{sub} in eV	E_{uvf} in eV	$\Omega_0 \kappa$ in eV	$\Omega_0 G$ in eV
Ag	17.10	2.85	1.10	11.10	3.61
Cu	11.81	3.54	1.30	10.17	4.05

In particular the following values can be used to obtain the second column of Table 1:

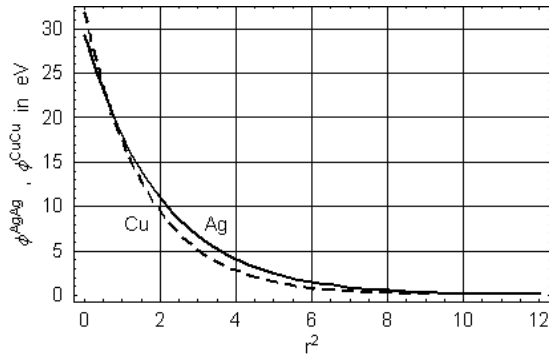
$$a^{\text{Ag}} = 4.09 \text{ \AA} \quad , \quad R^{\text{Ag}} = 2.89 \text{ \AA} \quad , \quad R^{\text{Ag}^2} = 8.36 \text{ \AA}^2 \quad (88)$$

$$a^{\text{Cu}} = 3.61 \text{ \AA} \quad , \quad R^{\text{Cu}} = 2.56 \text{ \AA} \quad , \quad R^{\text{Cu}^2} = 6.53 \text{ \AA}^2 \quad (89)$$

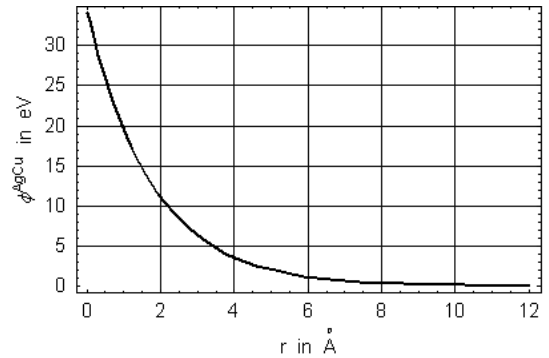
From this data the parameters and corresponding functions shown in Table 2 and in Figure 6 were obtained.

Table 2: Calculated parameters for Ag and Cu

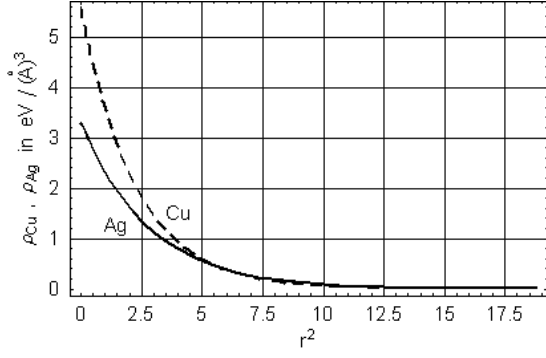
atom	α	β	γ	ϕ_e in eV	ρ_e in $\text{eV}/\text{\AA}^3$	$\bar{\rho}_e$ in $\text{eV}/\text{\AA}^3$
Ag	5.9205	2.9799	4.1300	0.4750	0.1672	2.0064
Cu	5.0849	2.9232	3.9966	0.5900	0.2998	3.5971



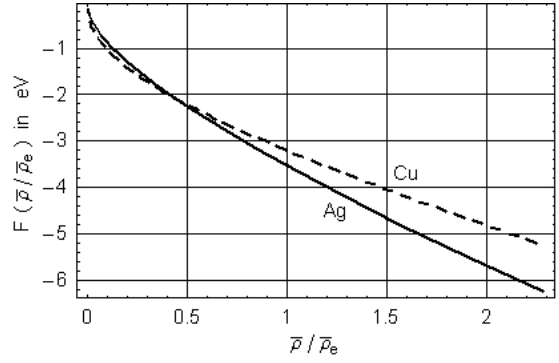
nucleus-nucleus interactions between atoms of the same type



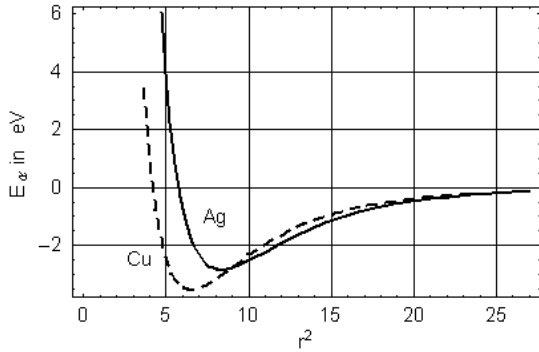
nucleus-nucleus interactions between atoms of different type



atomic electron-density for a silver and a copper atom



embedding function for a silver and a copper atom



atomic energy for a silver and a copper atom

Figure 6: Various functions relevant in Eq (74,77) and the resulting atomic energy E_α for Ag and Cu. Note that in the upper right picture holds $\phi^{\text{AgCu}} = \phi^{\text{CuAg}}$.

5.2 The elastic constants of Ag and Cu

With the fitted and illustrated functions from the last section it becomes possible to calculate the elastic constants for pure Ag and Cu according to Eq (30a). The results are compiled in Table 3.

In comparison with the results obtained by means of pair potentials [1] the discrepancy between experimental data and theoretically predicted values is visibly reduced and the agreement is reasonably good, the error ranging between 4.1% (C_{1122}^{Ag}) and 9.4% (C_{1111}^{Cu}). Moreover the CAUCHY-Paradox ($C_{1122} = C_{2323}$) no longer exists which is a considerable improvement.

5.3 The alloy Ag-Cu I: Evaluation of the equilibrium condition

In this section we investigate the equilibrium condition shown in Eq (65). We choose A=Ag and B=Cu and the corresponding equilibrium concentrations $c^\alpha = 0.063$ and $c^\beta = 0.945$ at 1000 K. Eq (65) has a nontrivial solution only for the index-pair $i = j$ since in an FCC lattice the following relation holds for an arbitrary scalar function f : $\sum f(R^2)R_iR_j = 0$, ($i \neq j$) and $\sum f(R^2)R_iR_i = \text{const}$, ($\forall i, j = \{1, 2, 3\}$). Consequently we may plot the left side (for the index 11) of Eq (65) as shown in Figure 7, left. The point of intersection with the abscissa defines the nearest neighbor distances in equilibrium of a crystal consisting of α or β phase, respectively.

On the other side it is possible to vary the concentration in the equilibrium condition (65) and determine the nearest neighbor distance in equilibrium as a function of the concentration c . The

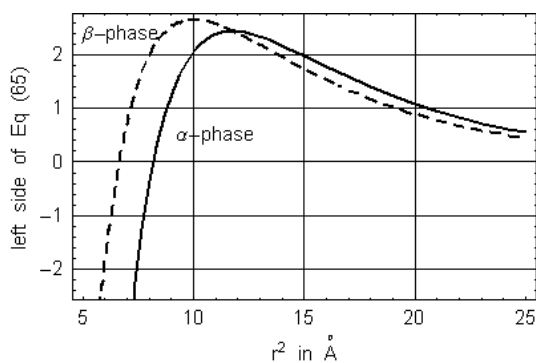
Table 3: Elastic constants for Ag and Cu in GPa. The values in parentheses are from experiments [20].

C_{ijkl}^{Ag}	kl	11	22	33	23	31	12	C_{ijkl}^{Cu}	kl	11	22	33	23	31	12
ij								ij							
11		132.6 (124)	90.2 (94)	90.2 (94)	0	0	0	11		183.7 (168)	115.1 (121)	115.1 (121)	0	0	0
22		90.2 (94)	132.6 (124)	90.2 (94)	0	0	0	22		115.1 (121)	183.7 (168)	115.1 (121)	0	0	0
33		90.2 (94)	90.2 (94)	132.6 (124)	0	0	0	33		115.1 (121)	115.1 (121)	183.7 (168)	0	0	0
23		0	0	0	42.4 (46)	0	0	23		0	0	0	68.7 (75)	0	0
31		0	0	0	0	42.4 (46)	0	31		0	0	0	0	68.7 (75)	0
12		0	0	0	0	0	42.4 (46)	12		0	0	0	0	0	68.7 (75)

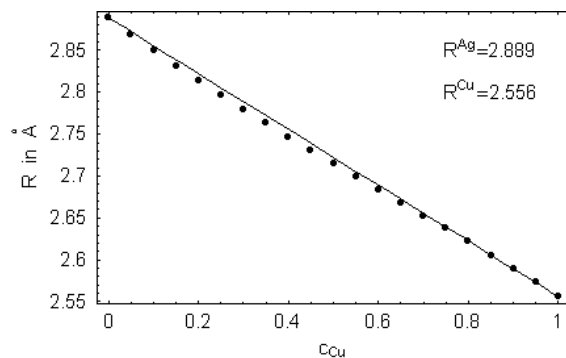
corresponding points of intersection were determined for various discrete concentrations $c = 0, 0.05, 0.10, \dots, 0.90, 0.95, 1$, cf., Figure 7, right. As one can see the obtained values of R are in good agreement with the weighed average $R = (1 - c)R^{\text{Ag}} + cR^{\text{Cu}}$ which is represented by the continuous line in Figure 7, right. Especially for the α - and β -phase we can conclude:

$$R^\alpha = \sqrt{8.202} \text{ \AA} = 2.864 \text{ \AA} \quad , \quad R^\beta = \sqrt{6.631} \text{ \AA} = 2.575 \text{ \AA} \quad , \quad (90)$$

$$\Omega_0^\alpha = 16.61 \text{ \AA}^3 \quad , \quad \Omega_0^\beta = 12.07 \text{ \AA}^3 \quad . \quad (91)$$



The equilibrium condition for the α - and β -phase ($i = j$)



Equilibrium nearest neighbor distances for different concentrations c .

Figure 7: Illustration of the different results followed from the exploitation of the equilibrium condition (65).

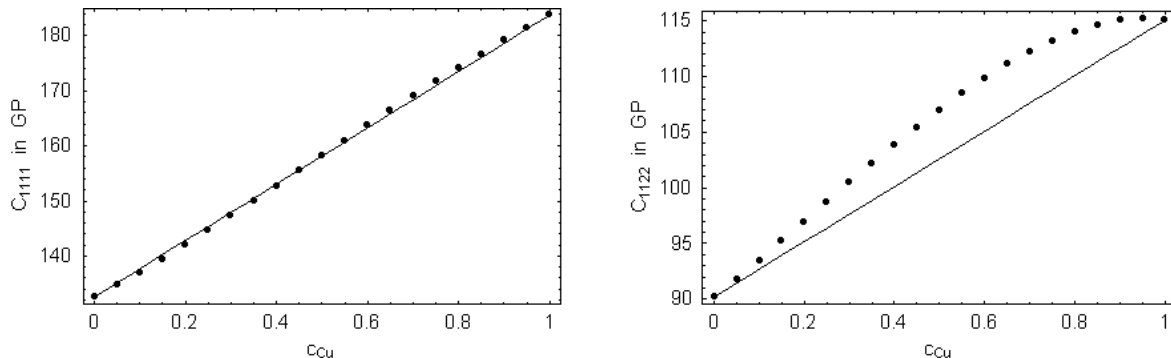
5.4 The alloy Ag-Cu II: The stiffness coefficients

Equation (66) allows us to obtain the stiffness coefficients as a function of the mass concentration c . Note that for every value of c one must first evaluate the equilibrium condition in order to find the nearest neighbor distance R in equilibrium. If R is determined for a certain value of c the unit cell volume Ω_0^α occupied by an atom α can be calculated. In order to investigate the stiffness of the different phases in Ag-Cu we consider the equilibrium concentrations c^α and c^β and analyze Eq (66) at the distances R^α and R^β presented in the previous section. The results are compiled in Table 4. On the other hand one can ask for the stiffness of the alloy

Table 4: Elastic constants in GPa predicted for the α - and β -phases in an Ag-Cu system at 1000 K.

C_{ijkl}^α	kl	11	22	33	23	31	12	C_{ijkl}^β	kl	11	22	33	23	31	12
ij								ij							
11		135.3	92.2	92.2	0	0	0	11		181.3	115.2	115.2	0	0	0
22		92.2	135.3	92.2	0	0	0	22		115.2	181.3	115.2	0	0	0
33		92.2	92.2	135.3	0	0	0	33		115.2	115.2	181.3	0	0	0
23		0	0	0	43.1	0	0	23		0	0	0	66.0	0	0
31		0	0	0	0	43.1	0	31		0	0	0	0	66.0	0
12		0	0	0	0	0	43.1	12		0	0	0	0	0	66.0

with an arbitrary mass concentration c . This question is equivalent to a somewhat hypothetical experiment in which the atoms of a pure Ag lattice are successively replaced by Cu atoms. For this purpose we use the calculated equilibrium distances R illustrated in Figure 7, right, and the corresponding concentrations values. The (discrete) values of the calculated stiffness coefficients are shown as bullets in Figure 8. Obviously the pure-substance-limit is exactly fulfilled, i.e.,



the elastic constants lead to C_{ijkl}^{Ag} and C_{ijkl}^{Cu} for $c = 0$ or $c = 1$, respectively.

5.5 The alloy Ag-Cu III: The higher gradient coefficients

In order to calculate the higher gradient coefficients for the strain-free case ($\mathbf{G} = \mathbf{0}$, for simplicity) we use the reduced form of Eq (71):

$$\mathbb{H}_{mn}(c, G_{ij} = 0) = \frac{1}{4} \left[(1 - 2y(c)) g_{mn}^\phi + g_{mn}^{\tilde{\phi}} \right] + \frac{1}{2} \bar{\rho}_{mn}^\Delta \left[F'_A + y(c) (F'_B - F'_A) \right]. \quad (92)$$

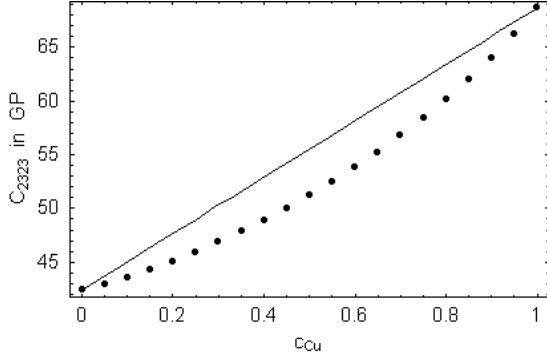


Figure 8: The calculated elastic constants for Ag-Cu as a function of the mass concentration c . The continuous line represent the linear interpolation between the values of pure Ag and Cu.

Furthermore the following data can be compiled for eutectic Ag-Cu:

$$\rho_{\text{Ag}} = 10490 \frac{\text{kg}}{\text{m}^3} \quad , \quad \rho_{\text{Cu}} = 8920 \frac{\text{kg}}{\text{m}^3} \quad , \quad \rho_0 = 9980.57 \frac{\text{kg}}{\text{m}^3} \quad , \quad \delta(c) = \frac{\rho_0}{\mu_0 M(c)}. \quad (93)$$

By applying $c^{\alpha/\beta}$ and $R^{\alpha/\beta}$ in Eqns (67,68,92,93₄) one can determine the higher gradient coefficients a_{ij} and b_{ij} for the α - and β -phase (cf., Table 5). Moreover, together with the calculated nearest neighbor distances in equilibrium which depend on c (Figure 7, right) we calculate $a_{ij}(c)$ and $b_{ij}(c)$ (cf., Figure 9). Note that for an FCC crystal we have $a_{ij} = b_{ij} = 0$ for $i \neq j$ and $a_{11} = a_{22} = a_{33}$ or $b_{11} = b_{22} = b_{33}$, respectively.

Table 5: Calculated higher gradient coefficients for the different α - and β -phases in eutectic Ag-Cu.

phase	a_{11} [N]	b_{11} [N]	A_{11} [N]	$\partial A_{11}/\partial c$ [N]
α	$4.59 \cdot 10^{-11}$	$6.14 \cdot 10^{-11}$	$1.55 \cdot 10^{-10}$	$7.34 \cdot 10^{-11}$
β	$1.23 \cdot 10^{-10}$	$1.03 \cdot 10^{-10}$	$1.88 \cdot 10^{-10}$	$2.86 \cdot 10^{-11}$

For the determination of $A_{ij}^{\alpha/\beta}$ or (more generally) $A_{ij}(c)$ and the corresponding derivative one has to find a closed form for the equilibrium distance $R^{\alpha/\beta} = R(c^{\alpha/\beta})$ or $R = R(c)$, respectively, first. Note that the derivatives $\partial a_{ij}/\partial c$, $\partial^2 a_{ij}/\partial c^2$ and $\partial b_{ij}/\partial c$ must be calculated and evaluated at the equilibrium distances R which also depends on c . Here we want to use the numerically obtained results from Section 5.3, i.e.,

$$R(c) \approx (1 - c)R^{\text{Ag}} + cR^{\text{Cu}}. \quad (94)$$

Now we can evaluate $A_{ij}^{\alpha/\beta}$ (cf., Table 5) as well as $A_{ij}(c)$ (cf., Figure 7) and the corresponding derivatives with respect to c . Analogously we have for FCC crystals $A_{ij} = 0$ for $i \neq j$ and $A_{11} = A_{22} = A_{33}$ for $i = j$.

6 Construction of the phase diagram

In order to point out the reliability of the predicted stiffness coefficients and the HGCs we want to calculate finally the equilibrium particle concentrations $y^{\alpha/\beta}$ for different temperatures using the EAM and compare them with experimental data. The resulting phase diagram represents the coexisting phases in the binary alloy at different temperatures.

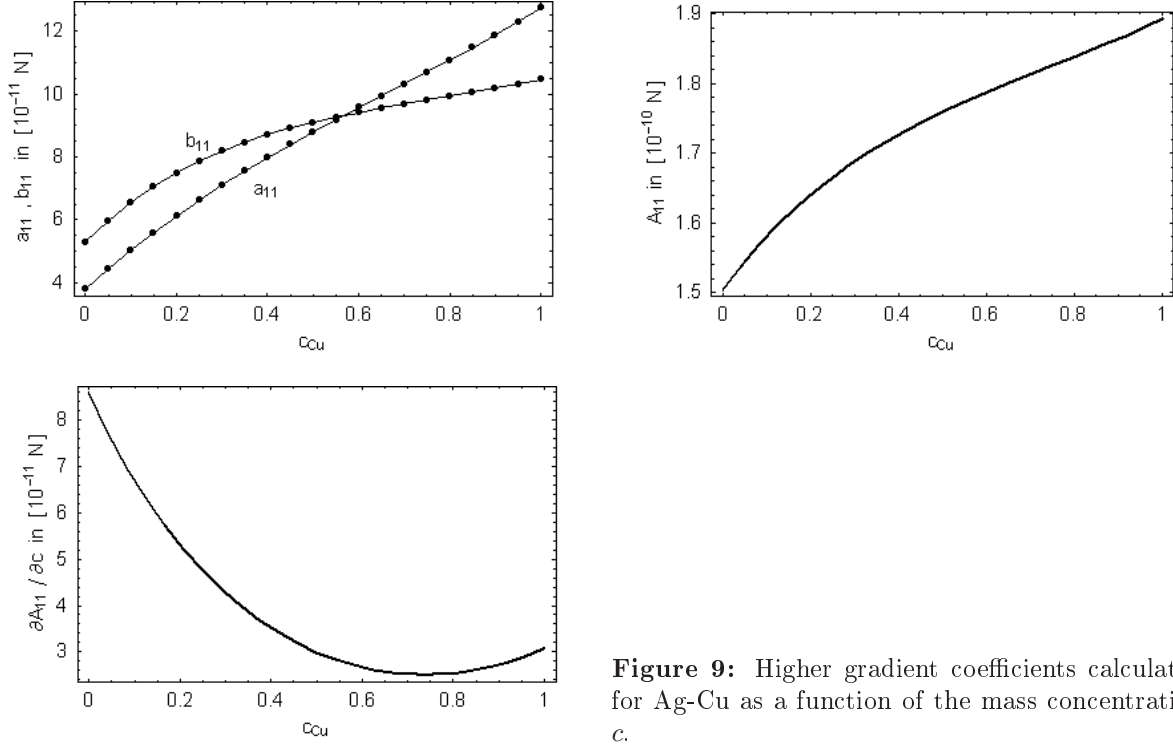


Figure 9: Higher gradient coefficients calculated for Ag-Cu as a function of the mass concentration c .

From (phenomenological) thermodynamics of mixtures it is well-known that the equilibrium concentrations of a binary mixture can be constructed from the GIBBS free energy $g(y, T)$, (pressure $p = \text{const}$) for a given temperature performing the MAXWELL *tangent construction*. Here the derivatives of the $g(y, T)$ -curve at the equilibrium concentrations $y^{\alpha/\beta}$ must be identical to the slope of the common tangent.

Starting from the atomistic point of view the GIBBS free energy $g(y, T)$ *per atom* can be identified according to Eq (64) as follows:

$$\begin{aligned}
 g(y, T) \equiv E_\alpha - Ts &= \frac{1}{2}g^{\text{AA}} + y(1-y)g^\phi + yg^{\tilde{\phi}} + F_A + y(F_B - F_A) - Ts \\
 &= (1-y)\left(6\phi^{\text{AA}}(R^2) + F_A(\bar{\rho}_{av}(R^2))\right) + y\left(6\phi^{\text{BB}}(R^2) + F_B(\bar{\rho}_{av}(R^2))\right) + \\
 &\quad + 12y(1-y)g^\phi(R^2) + k_B T\left(y \ln y + (1-y) \ln(1-y)\right). \quad (95)
 \end{aligned}$$

Here the temperature-dependence of $g(y, T)$ is only characterized by the entropic part, namely by $-Ts$. Furthermore the MAXWELL tangent construction reads:

$$\left. \frac{\partial g(y, T)}{\partial y} \right|_{y=y^\alpha} = \left. \frac{\partial g(y, T)}{\partial y} \right|_{y=y^\beta} = \frac{g(y^\beta, T) - g(y^\alpha, T)}{y^\beta - y^\alpha}. \quad (96)$$

Note that in Eq (95) all terms, i.e., g^{AA} , g^ϕ , $g^{\tilde{\phi}}$ and $F_{A/B}$ depend on the equilibrium nearest neighbor distance R^2 which is a function of the mass concentration c (c.f., Eq (94)). In order to find $R = R(y)$ one can use the inverse relation $c = c(y)$ of Eq (113):

$$c_{\text{Cu}} \equiv c = \frac{m_{\text{Cu}}}{m_{\text{Cu}} + m_{\text{Ag}}} = \frac{yM_{\text{Cu}}}{yM_{\text{Cu}} + (1-y)M_{\text{Ag}}}. \quad (97)$$

In a same manner one can analyze the GIBBS free energy density $\psi(c, T) = g(y(c), T)/\delta(c)$ as a function of the mass concentration c . Then the resulting equilibrium concentrations are represented by $c^{\alpha/\beta}$ in the phase diagram. Both approaches are equivalent and y can be transferred to c through Eq (97). *Here we want to investigate $g(y, T)$ and calculate the equilibrium concentrations $y^{\alpha/\beta}$ as well as the according phase diagram due to a better comparison with experimental/literature data.*

Figure 10 shows the particle-specific GIBBS free energy for the temperature 1000 Kelvin following from Eq. (95) and the according ψ -curve (1st row) as well as the relation $R(y)$ (2nd row).

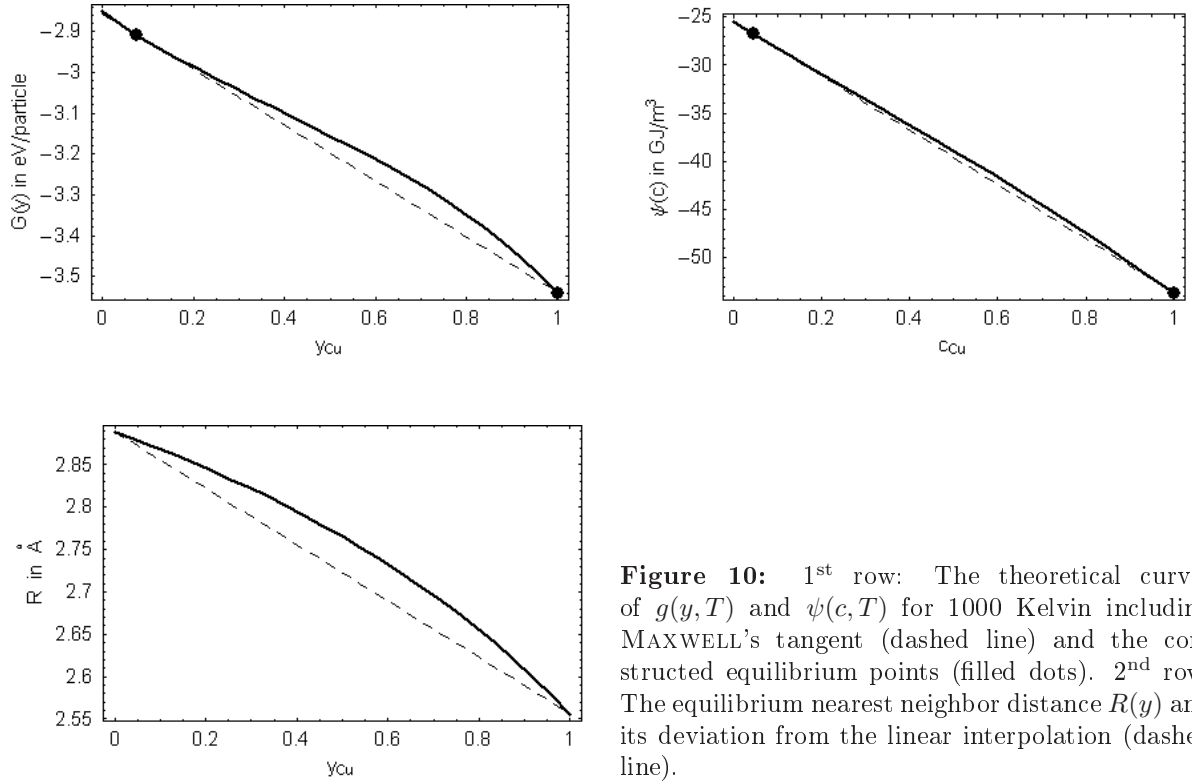


Figure 10: 1st row: The theoretical curves of $g(y, T)$ and $\psi(c, T)$ for 1000 Kelvin including MAXWELL's tangent (dashed line) and the constructed equilibrium points (filled dots). 2nd row: The equilibrium nearest neighbor distance $R(y)$ and its deviation from the linear interpolation (dashed line).

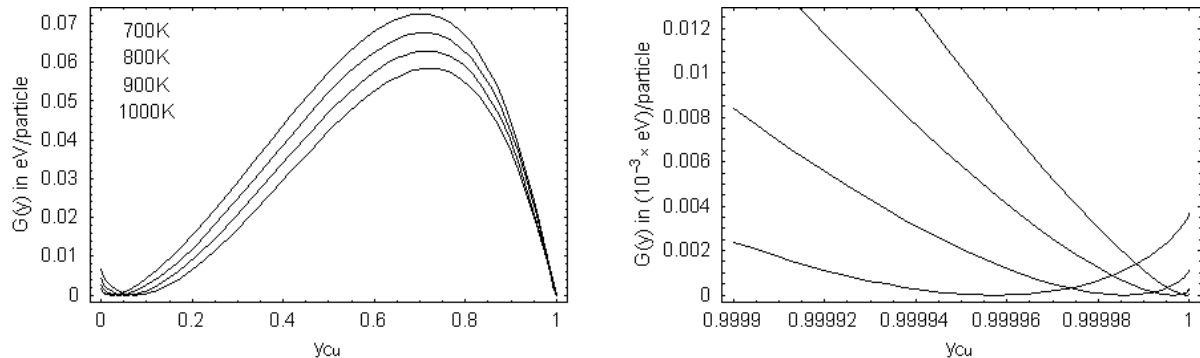
Note that the ψ -curves of Figure 5 and Figure 10 can not be directly compared due to different zero points on the energy scale.

Evaluating Eq (95) for different temperatures, in particular for 700, 800, 900, and 1000 Kelvin yields the curves illustrated in Figure 11 (1st row). Here MAXWELL's tangent is removed from the values of g . Thus the minima of these functions represent the equilibrium concentrations for the according temperature. Note that there are also minima on the "right side" of the curve, pointed out by the zoomed right picture. Furthermore the calculated and experimental equilibrium concentrations $y_{\alpha/\beta}$ and $c_{\alpha/\beta}$ are confronted in Table 6. The resulting (theoretically determined) phase diagram one can find in Figure 11 (2st row, left). The full diagram on the right side is the according one obtained from MTdataTM, [18]. A comparison of the values in Table 6 as well as the theoretical and experimental phase diagram shows that the theoretically predicted equilibrium concentrations have qualitatively the same tendency as the experimental ones. Furthermore the absolute values of the α -phase (left part of the phase diagram) are in good agreement but, nevertheless, the values of the β -phase are poorly reproduced.

Let us abbreviate the difference of GIBBS free energy $g(y, T)$ and Maxwells's tangent with $g^*(y, T)$

Table 6: Calculated and experimental equilibrium concentrations for Ag-Cu at different temperatures. The experimental data for 700, 800, 900 Kelvin are from [22] and for 1000 Kelvin from [15].

Temp. in Kelvin	predicted by EAM				experimental data			
	y_α	y_β	c_α	c_β	y_α	y_β	c_α	c_β
700	0.024	0.999999	0.014	0.999999	0.015	0.993	0.0089	0.9882
800	0.039	0.999996	0.023	0.999994	0.033	0.986	0.0197	0.9765
900	0.056	0.999986	0.033	0.999976	0.063	0.976	0.0381	0.9599
1000	0.075	0.999957	0.045	0.999928	0.102	0.967	0.0627	0.9452



(cf., Figure 11, 1st row) and the according values of $\psi(c, T)$ with $\psi^*(c, T)$. For the investigation of the source of deviation between the experimental and calculated equilibrium concentrations one can now compare $g^*(y, T = 1000\text{K})$ as well as $\psi^*(c, T = 1000\text{K})$ following from the atomistic calculations and from the MTdataTM database. Moreover, it is also possible to calculate the so-called Excess-enthalpy g^{ex} , the non-ideal heat of mixing, which can be obtained from the following relation:

$$g(y, T) = yg(y = 0, T) + (1 - y)g(y = 1, T) + k_B T \left(y \ln y + (1 - y) \ln(1 - y) \right) + g^{\text{ex}}(y, T). \quad (98)$$

Figure 12 shows the confronted curves for 1000 Kelvin. Obviously the crucial value that determines the quality of the calculated phase diagram is the excess enthalpy g^{ex} . In particular, its asymmetry is the source of the asymmetry in the phase diagram related to the solid state and its absolute values compete with the entropic part $-Ts$ and determines the horizontal position of the minima of g^{mix} . Thus values of g^{ex} that are too large lead to a shift of the minima (and, consequently, of the equilibrium concentrations) in the vicinity of $y = 0$ or $y = 1$, respectively. This fact is observable in our theoretical calculations, where the calculated g^{ex} is considerably larger than the experimental curve, but, nevertheless, have the same magnitude and the same functional characteristics (asymmetry) as the other curves. The source of the deviation of g^{ex} is due to the use of the calculated nearest neighbor distance R in equilibrium, a measure for the relaxation of the lattice caused by different atom-types. This value can only be as realistic as the (fitted) EAM potentials, because they enter the equilibrium condition used to find R . In spite of these shortcomings our phase diagram calculations, first, qualitatively reproduce the experimental values and, second, are of the same magnitude as the literature data.

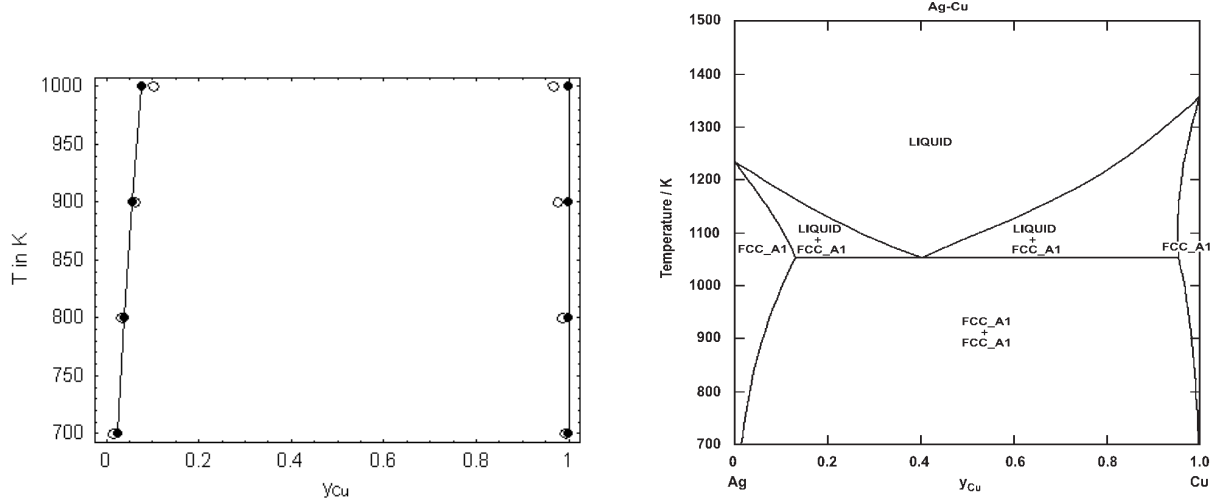
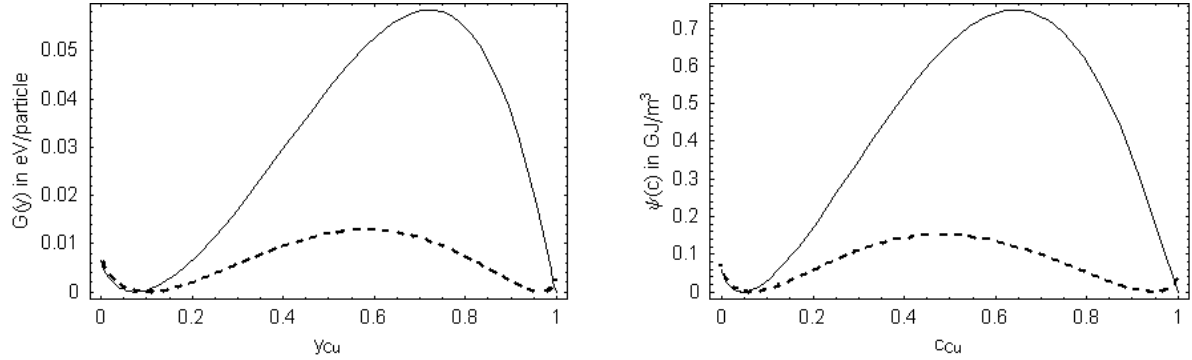


Figure 11: 1st row: The calculated GIBBS free energy $g(y, T)$ for the different temperatures 700, 800, 900, 1000 Kelvin. 2nd row, left : The calculated solid part of the phase diagram of Ag-Cu (filled and joined dots) vs. experimental data (unfilled dots). Right: The phase diagram generated by MTdataTM.



7 Conclusion and Outlook

A compact theory was presented which allows for an atomistic identification of mechanical, thermodynamical as well as thermo-mechanical material parameters in binary alloys. It is based on EAM potentials and results in an energy expression for an arbitrary atom α , given by Eq (64). Undoubtedly this equation represents the central element in the outlined procedure and is generally valid, i.e., it does not depend on the functional form of the EAM-functions.

By considering a binary (multiphase) mixture the equilibrium (atomic) nearest neighbor distance R , the stiffness coefficients, the higher gradient coefficients, and the (temperature-depending) equilibrium concentrations of the different phases can easily be calculated. Moreover it is also possible to determine these quantities as (continuous) functions of mass or particle concentrations c and y , respectively. Furthermore the equilibrium condition following from Eq (64) represents the energy-minimization-principle and provides a theoretical tool for an estimate of lattice relaxations due to different atom-types in the lattice.

However, the main focus of this paper was the theoretical description of the HGCs, since so far the communicated data are mostly estimated or their origin is not clear. That is why the existing data are questionable. In order to substantiate the reliability of the predicted HGCs we

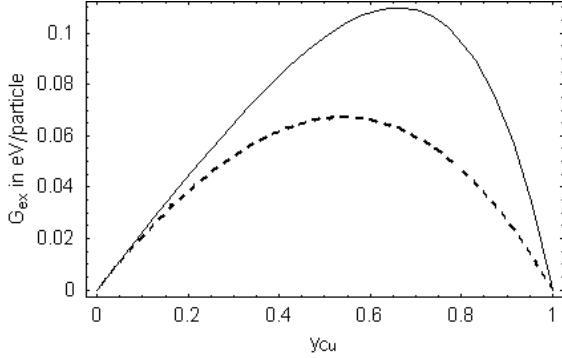


Figure 12: A comparison of the calculated $g^*(y, T = 1000\text{K})$, $\psi^*(c, T = 1000\text{K})$, and $g^{\text{ex}}(y, T = 1000\text{K})$ functions with the according functions obtained from MTdataTM (dashed line).

also determined the stiffness coefficients and constructed the solid part of the phase diagram. Especially we chose the binary alloy Ag-Cu for the illustration of the theoretical determination of the above mentioned parameters.

For the whole investigation the nearest neighbor model as proposed by Johnson [3] was used. This special form considers a very simple functional dependence for the EAM functions, assuming only nearest neighbor interactions and s-orbitals for the electron sheath. Nevertheless, the determined quantities, for instance the stiffness coefficients, are in good agreement with the experimental data. Only the calculated equilibrium concentrations in the phase diagram partially inaccurately reproduce the experimental values. It seems that Johnson's parametrization only allows a qualitative calculation of phase diagram data. Here one could use other functional forms or extensions of Johnson's model. One possibility is to consider more neighboring atoms as suggested by Daw and Baskes in [13].

Moreover new modifications of EAM were developed in the last years in order to apply this method to other than FCC lattices [24, 25]. As an example the Modified Embedded-Atom Method (MEAM) allows the investigation of BCC-metals, for instance Fe. HCP structures were also investigated successfully with EAM [26]. Therefore, in principle, it is possible to determine the HGCs of more complex lattice structures using EAM/MEAM. Other applications of the EAM, which could be interesting in the future are simulations and investigations of fracture, plasticity behavior, impurities, surfaces or grain boundaries.

In summary one can say that the predicted HGCs originated from a microscopic theory based on interatomic interactions are reliable as indicated by the quality of the stiffness coefficients and (despite of some deviations) by the phase diagram construction. Indeed, the value of A_{ij} is close to those found in literature (e.g., [27], $A_{ij} = 2 \cdot 10^{-10} \delta_{ij}$ N). An investigation of the influence of the calculated HGCs on phase separation and the coarsening processes in binary alloys according to Eq (2) is currently underway and will be published in a subsequent paper.

Appendix A. The extended diffusion equation

In the Appendix of [2] Dreyer and Müller presented a derivation of an extended diffusion equation by means of Rational Thermodynamics. They started from the classical (5 field) partial balance equation of *mass*, *momentum*, and *internal energy* using a LAGRANGEian description. Furthermore they chose the following state space Z :

$$Z = \left\{ T, c, \frac{\partial c}{\partial X_i}, \frac{\partial^2 c}{\partial X_i \partial X_j}, \varepsilon_{ij} \right\} \quad (99)$$

by means of which all constitutive quantities (e.g., diffusion flux J_i , heat flux Q_k , and first or second PIOLA-KIRCHHOFF stress tensor, t_{ik} or T_{ik}) follow. The balance equations become field equations if the constitutive equations are inserted, which link the elements of the state space to the constitutive quantities in a material-dependent manner. In order to take the second law of thermodynamics into account Dreyer and Müller applied Liu's method [21]. The local entropy inequality

$$\rho_0 \frac{ds}{dt} + \frac{\partial \phi_k}{\partial X_k} = \Sigma \geq 0 \quad (100)$$

(s being the entropy, ϕ_k the entropy flux, and Σ the (positive) entropy production density) holds for all processes that are solutions to the field equations. If the balance equations are interpreted as constraints, i.e., multiplied by LAGRANGE factors Λ^c , Λ_i^v , Λ^u and added to Eq (100) the inequality is then valid for arbitrary fields and can be exploited. This procedure leads to following extended diffusion equation [2]:

$$\rho_0 \frac{\partial c}{\partial t} + \frac{\partial J_i}{\partial X_i} = 0 \quad \text{and} \quad J_i = -\rho_0 M_{ij} \frac{\partial \Lambda^c}{\partial X_j}. \quad (101)$$

Here Λ^c refers to the mass balance and can be identified with the chemical potential μ . Moreover it holds in accordance with the second law of thermodynamics, [11] we find that:

$$\Lambda^c \equiv \mu = \frac{\partial \psi}{\partial c} - \frac{\partial}{\partial X_m} \left(\frac{\partial \psi}{\partial (\partial c / \partial X_m)} \right) + \frac{\partial^2}{\partial X_m \partial X_n} \left(\frac{\partial \psi}{\partial (\partial^2 c / \partial X_m \partial X_n)} \right) \quad (102)$$

where ψ represents the GIBBS free energy density. Following Cahn and Hilliard on p. 259 in [6] a system with an inhomogeneous mass-concentration profile $c(X_i, t)$ can be characterized by the equation:

$$\psi = \psi_{\text{conf}}(c, \varepsilon_{ij}) - a_{kl}(c, \varepsilon_{ij}) \frac{\partial^2 c}{\partial X_k \partial X_l} + b_{kl}(c, \varepsilon_{ij}) \frac{\partial c}{\partial X_k} \frac{\partial c}{\partial X_l}. \quad (103)$$

The last term of the right side of Eq (103) was neglected by Dreyer and Müller as well as in various other publications and represents a more general case. Finally the first term $\psi_{\text{conf}}(c, \varepsilon_{ij})$ is the contribution of a solution with a homogeneous concentration profile and consists of two parts:

$$\psi_{\text{conf}}(c, \varepsilon_{ij}) = \psi_0(c) + \frac{1}{2}(\varepsilon_{ij} - \varepsilon_{ij}^*) C_{ijkl} (\varepsilon_{kl} - \varepsilon_{kl}^*), \quad (104)$$

where $\psi_{\text{elast}} = 1/2(\varepsilon_{ij} - \varepsilon_{ij}^*) C_{ijkl} (\varepsilon_{kl} - \varepsilon_{kl}^*)$ denotes the energy density due to elastic, eigen- and thermal strains.

In order to obtain the extended diffusion equation (2) we have to calculate the expressions $\partial \psi / \partial c$, $-\partial \psi / \partial (\partial c / \partial X_m)$, and $\partial \psi / \partial (\partial^2 c / \partial X_m \partial X_n)$ in Eq (102) using ψ as given by (103):

$$\frac{\partial \psi}{\partial c} = \frac{\partial \psi_{\text{conf}}(c, \varepsilon_{ij})}{\partial c} - \frac{\partial a_{kl}(c, \varepsilon_{ij})}{\partial c} \frac{\partial^2 c}{\partial X_k \partial X_l} + \frac{\partial b_{kl}(c, \varepsilon_{ij})}{\partial c} \frac{\partial c}{\partial X_k} \frac{\partial c}{\partial X_l}, \quad (105)$$

$$-\frac{\partial \psi}{\partial (\partial c / \partial X_m)} = -2b_{ml} \frac{\partial c}{\partial X_l}, \quad \frac{\partial \psi}{\partial (\partial^2 c / \partial X_m \partial X_n)} = -a_{kl}. \quad (106)$$

Consequently it follows by means of the chain rule:

$$-\frac{\partial}{\partial X_m} \left(\frac{\partial \psi}{\partial (\partial c / \partial X_m)} \right) = -2 \left(\frac{\partial b_{ml}}{\partial c} \frac{\partial c}{\partial X_m} \frac{\partial c}{\partial X_l} + \frac{\partial b_{ml}}{\partial \varepsilon_{rs}} \frac{\partial \varepsilon_{rs}}{\partial X_m} \frac{\partial c}{\partial X_l} + b_{ml} \frac{\partial^2 c}{\partial X_m \partial X_l} \right), \quad (107)$$

$$\begin{aligned} \frac{\partial^2}{\partial X_m \partial X_n} \left(\frac{\partial \psi}{\partial (\partial^2 c / \partial X_m \partial X_n)} \right) &= - \left(\frac{\partial^2 a_{mn}}{\partial c^2} \frac{\partial c}{\partial X_m} \frac{\partial c}{\partial X_n} + \frac{a_{mn}}{\partial c} \frac{\partial^2 c}{\partial X_m \partial X_n} + \right. \\ &\quad \left. + 2 \frac{\partial^2 a_{mn}}{\partial c \partial \varepsilon_{rs}} \frac{\partial \varepsilon_{rs}}{\partial X_m} \frac{\partial c}{\partial X_n} + \frac{\partial^2 a_{mn}}{\partial \varepsilon_{op} \varepsilon_{rs}} \frac{\partial \varepsilon_{op}}{\partial X_m} \frac{\partial \varepsilon_{rs}}{\partial X_n} + \frac{\partial a_{mn}}{\partial \varepsilon_{rs}} \frac{\partial^2 \varepsilon_{rs}}{\partial X_m \partial X_n} \right) \end{aligned} \quad (108)$$

By applying the results of Eqns (105-108) as well as the definition:

$$A_{ij} = \frac{\partial a_{ij}}{\partial c} + b_{ij} \quad (109)$$

to Eq (102) the following relation is obtained:

$$\begin{aligned} \mu &= \frac{\partial \psi_{\text{conf}}}{\partial c} - 2A_{kl} \frac{\partial^2 c}{\partial X_k \partial X_l} - \frac{\partial A_{kl}}{\partial c} \frac{\partial c}{\partial X_k} \frac{\partial c}{\partial X_l} \\ &\quad - 2 \frac{\partial A_{kl}}{\partial \varepsilon_{mn}} \frac{\partial c}{\partial X_k} \frac{\partial \varepsilon_{mn}}{\partial X_l} - \frac{\partial^2 a_{kl}}{\partial \varepsilon_{op} \varepsilon_{mn}} \frac{\partial \varepsilon_{op}}{\partial X_k} \frac{\partial \varepsilon_{mn}}{\partial X_l} - \frac{\partial a_{kl}}{\partial \varepsilon_{mn}} \frac{\partial^2 \varepsilon_{mn}}{\partial X_k \partial X_l}. \end{aligned} \quad (110)$$

The combination of Eq (110) and Eq (101)₂ results in Eq (2). The quantities a_{ij} , b_{ij} and A_{ij} are called Higher Gradient Coefficients (HGCs) and can be identified with the quantities $-\kappa_1$, κ_2 and κ introduced by Cahn and Hilliard in [6] on p. 259.

Appendix B. Conversion of particle to mass concentration

The total Gibbs free energy of an equilibrium phase γ follows by summation from Eq (64):

$$\begin{aligned} G^\gamma &= \sum_{\alpha \in \gamma} E_\alpha - TS^\gamma, \quad S^\gamma = -k_B \sum_{\alpha \in \gamma} [y \ln y + (1-y) \ln(1-y)], \\ E_\alpha &\stackrel{(64)}{=} \frac{1}{2} g^{\text{AA}} + y(1-y)g^\phi + yg^{\tilde{\phi}} + F_A + y(F_B - F_A) + \\ &\quad + \frac{1}{2} G_{ij} G_{kl} \{ \dots \}_{ijkl}(y) + (\nabla_{mn}^2 y) \{ \dots \}_{mn}(y), \end{aligned} \quad (111)$$

where $\{ \dots \}_{ijkl}$ and $\{ \dots \}_{mn}$ represent the expressions within the brackets of the second and third block in Eq (64). Furthermore k_B denotes Boltzmann's constant and TS^γ the entropic part of G^γ . Moreover, the sum is carried out with respect to all particles α of the phase γ , and E_α represents the energy of a particle due to its interactions with the neighbors β . The quantities g^{AA} , g^ϕ , $g^{\tilde{\phi}}$, F_A , F_B , $\{ \dots \}_{ijkl}$, and $\{ \dots \}_{mn}$ are defined by means of the EAM potentials (cf., Eq (64)) determined by the distance $R^{\alpha\beta^2}$ between atom α and β . In order to obtain the stiffness coefficients and the HGCs as functions of c the following procedure is performed:

1. Relate the ‘‘macroscopic’’ Gibbs free energy density ψ to the microscopic equation (111).
2. Substitute the derivatives of the particle concentration y for terms of the mass concentration c . Here one can use the relation:

$$c_B = (1 - c_A) \equiv c = \frac{m_B}{m_B + m_A} = \frac{y_B M_B}{y_B M_B + (1 - y_B) M_A} \quad (112)$$

$$\Rightarrow y_B = (1 - y_A) \equiv y = \tilde{y}(c) = \frac{c M_A}{M_B - c(M_B - M_A)}, \quad (113)$$

where $M_{A/B}$ is the molecular weight of the components A/B, and c_B is the mass concentration of B.

3. Compare the resulting equations with the macroscopic equations (62,63) and identify the HGCs and stiffness coefficients.

We recall the following thermodynamical relations for one Mole:

$$\hat{G} = N_A(E_\alpha - Ts) \quad , \quad \psi = \rho_0 \frac{\hat{G}}{m} \quad , \quad m = N_A \mu_0 M(c) \quad , \quad (114)$$

$$\Rightarrow \psi = \delta(c)(E_\alpha - Ts) \quad \text{with} \quad \delta(c) = \frac{1}{\Omega_0(c)} = \frac{\rho_0}{\mu_0 M(c)} \quad \text{and} \quad \frac{1}{\rho_0} = \frac{c_0}{\rho_{Cu}} + \frac{1-c_0}{\rho_{Ag}} \quad . \quad (115)$$

\hat{G} stands for the Gibbs free energy per one Mole, $N_A = 6.0237 \cdot 10^{23}$ is the number of particles in one Mole (AVOGADRO's constant) and $s = -k_B[y \ln y + (1-y) \ln(1-y)]$ represents the entropy with respect to one particle. Furthermore m denotes the total mass, ρ_0 identifies the mass density of the alloy in the homogeneous reference state with the (homogeneous) concentration c_0 and $\mu_0 = 1.66 \cdot 10^{-27}$ kg stands for $\frac{1}{12}$ of the weight of a Carbon 12 atom. The symbol $M(c)$ denotes an averaged molecular weight of the binary alloy A-B and can be obtained from the molecular weights of the pure components through the relation $M = \tilde{M}(c) = y(c)M_B + [1-y(c)]M_A$. The symbol δ identifies the reciprocal volume occupied by an atom and yields the following expression:

$$\begin{aligned} \frac{1}{\delta(c)}\psi &= \frac{1}{2}g^{AA} + y(1-y)g^\phi + yg^{\tilde{\phi}} + F_A + y(F_B - F_A) + \\ &+ \frac{1}{2}G_{ij}G_{kl} \{ \dots \}_{ijkl}(y) + (\nabla_{mn}^2 y) \{ \dots \}_{mn}(y) + k_B T [y \ln y + (1-y) \ln(1-y)] \end{aligned} \quad (116)$$

Considering the function $\tilde{y}(c)$ in Eq (113) and applying the chain rule one can replace $\nabla_{mn}^2 y$ with the following relation:

$$\begin{aligned} \nabla_{mn}^2 y &= \frac{\partial^2 y}{\partial c^2} \frac{\partial c}{\partial X_m} \frac{\partial c}{\partial X_n} + \frac{\partial y}{\partial c} \frac{\partial^2 c}{\partial X_m \partial X_n} \\ &= \frac{2M_A M_B (M_B - M_A)}{[M_B - (M_B - M_A)c]^3} (\nabla_m c)(\nabla_n c) + \frac{M_A M_B}{[M_B - (M_B - M_A)c]^2} \nabla_{mn}^2 c \end{aligned} \quad (117)$$

$$\equiv \mathbf{M}(c) \cdot \mathcal{D}_{mn}(c) \quad , \quad (118)$$

with the symbolic notation for the vector $\mathbf{M}(c)$ and for the vectorial differential operator $\mathcal{D}_{mn}(\diamond)$ as follows:

$$\begin{aligned} \mathbf{M}(c) &= \begin{pmatrix} M^{(1)}(c) \\ M^{(2)}(c) \end{pmatrix} = \begin{pmatrix} \frac{2M_A M_B (M_B - M_A)}{[M_B - (M_B - M_A)c]^3} \\ \frac{M_A M_B}{[M_B - (M_B - M_A)c]^2} \end{pmatrix} \quad \text{and} \\ \mathcal{D}_{mn}(\diamond) &= \begin{pmatrix} \mathcal{D}_{mn}^{(1)} \\ \mathcal{D}_{mn}^{(2)} \end{pmatrix} = \begin{pmatrix} \nabla_m(\diamond) \nabla_n(\diamond) \\ \nabla_{mn}^2(\diamond) \end{pmatrix} \quad . \end{aligned} \quad (119)$$

A combination of the relations (113,117) with Eq (116) yields the following expressions:

$$\frac{\psi_0(c)}{\delta(c)} = \frac{1}{2}g^{\text{AA}} + y(c)(1 - y(c))g^\phi + y(c)g^{\tilde{\phi}} + F_A + y(c)(F_B - F_A), \quad (120)$$

$$\frac{\psi_{\text{elast}}(c)}{\delta(c)} = E_{\text{elast}}^\alpha = \frac{\Omega_0^\alpha}{2}G_{ij} C_{ijkl}(c) G_{kl}, \quad (121)$$

$$\frac{a_{mn}(c, G_{pq})}{\delta(c)} = -M^{(2)}(c) \mathbb{H}_{mn}(c, G_{pq}), \quad (122)$$

$$\frac{b_{mn}(c, G_{pq})}{\delta(c)} = M^{(1)}(c) \mathbb{H}_{mn}(c, G_{pq}), \quad (123)$$

$$\begin{aligned} C_{ijkl}(c) = & \frac{1}{\Omega_0^\alpha} \left[2B_{ijkl}^\text{A} + 4y(c)(1 - y(c))B_{ijkl}^\phi + 4y(c)B_{ijkl}^{\tilde{\phi}} + 4(W_{ijkl}^\text{A} + y(c)W_{ijkl}^\Delta) \times \right. \\ & \left. \times (F'_\text{A} + y(c)(F'_\text{B} - F'_\text{A})) + 4(V_{ij}^\text{A} + y(c)V_{ij}^\Delta)(V_{kl}^\text{A} + y(c)V_{kl}^\Delta)(F''_\text{A} + y(c)(F''_\text{B} - F''_\text{A})) \right], \end{aligned} \quad (124)$$

$$\begin{aligned} \mathbb{H}_{mn}(c, G_{pq}) = & \frac{1}{4} \left((1 - 2y(c))g_{mn}^\phi + g_{mn}^{\tilde{\phi}} \right) + \frac{1}{2}\bar{\rho}_{mn}^\Delta (F'_\text{A} + y(c)(F'_\text{B} - F'_\text{A})) \\ & + \frac{1}{2}G_{ij} \left[(1 - 2y(c))A_{ijmn}^\phi + A_{ijmn}^{\tilde{\phi}} + 2V_{ijmn}^\Delta (F'_\text{A} + y(c)(F'_\text{B} - F'_\text{A})) \right. \\ & \left. + 2\bar{\rho}_{mn}^\Delta (V_{ij}^\text{A} + y(c)V_{ij}^\Delta)(F''_\text{A} + y(c)(F''_\text{B} - F''_\text{A})) \right] \\ & + \frac{1}{2}G_{ij}G_{kl} \left[(1 - 2y(c))B_{ijklmn}^\phi + B_{ijklmn}^{\tilde{\phi}} \right. \\ & + 2W_{ijklmn}^\Delta (F'_\text{A} + y(c)(F'_\text{B} - F'_\text{A})) + 2\bar{\rho}_{mn}^\Delta (W_{ijkl}^\text{A} + y(c)W_{ijkl}^\Delta)(F''_\text{A} + y(c)(F''_\text{B} - F''_\text{A})) \\ & + 2V_{klmn}^\Delta (V_{ij}^\text{A} + y(c)V_{ij}^\Delta)(F''_\text{A} + y(c)(F''_\text{B} - F''_\text{A})) + 2V_{ijmn}^\Delta (V_{kl}^\text{A} + y(c)V_{kl}^\Delta) \times \\ & \left. \times (F''_\text{A} + y(c)(F''_\text{B} - F''_\text{A})) + 2\bar{\rho}_{mn}^\Delta (V_{ij}^\text{A} + y(c)V_{ij}^\Delta)(V_{kl}^\text{A} + y(c)V_{kl}^\Delta)(F'''_\text{A} + y(c)(F'''_\text{B} - F'''_\text{A})) \right]. \end{aligned} \quad (125)$$

The HGCs A_{kl} can directly be calculated from (122) and (123) by means of the relation $A_{kl} = \frac{\partial a_{kl}}{\partial c} + b_{kl}$. Moreover it should be mentioned that Eqns (120-123) hold for a equilibrium phase consisting of two components in which the composition is characterized by the mass concentration $c \equiv c_B$.

Appendix C. Two equations for G and for E_{uvf}

We consider the Eqns (81) and (30a) together with the definitions shown in Eqns (82-85). In order to determine the coefficients C_{1111} , C_{1122} , and C_{2323} we first calculate all the required

derivatives:

$$\rho'(R^2) = -\beta \frac{\rho_e}{R^2} \quad , \quad \rho''(R^2) = \beta^2 \frac{\rho_e}{R^4} \quad , \quad \phi'(R^2) = -\gamma \frac{\phi_e}{R^2} \quad , \quad \phi''(R^2) = \gamma^2 \frac{\phi_e}{R^4} \quad (126)$$

$$F'(\bar{\rho}_e) = -6 \frac{\gamma \phi_e}{\beta \bar{\rho}_e} \quad , \quad F''(\bar{\rho}_e) = \frac{E_{\text{sub}} \alpha^2 + 24 \gamma \phi_e (\beta - \gamma)}{4 \beta^2 \bar{\rho}_e^2}. \quad (127)$$

Due to nearest neighbor interactions all neighbors of an atom α are separated by the same distance R . Thus the derivatives ρ' , ρ'' , and ϕ'' do not depend on the sum and one can write for a pure substance:

$$C_{ijkl} = \frac{1}{\Omega_0} \left[2\phi'' \left(\sum_{\beta} R_i R_j R_k R_l \right) + 4F' \rho'' \left(\sum_{\beta} R_i R_j R_k R_l \right) + 4F'' \rho' \rho' \left(\sum_{\beta} R_i R_j \right) \left(\sum_{\beta} R_k R_l \right) \right] \quad (128)$$

Note that for an FCC crystal the following relations hold: $\sum R_1^4 = 8(a/2)^4$, $\sum R_1^2 = \sum R_2^2 = 8(a/2)^2$, $\sum R_2^2 R_3^2 = 4(a/2)^2 (a/2)^2$, and $\sum R_2 R_3 = 0$, cf., Figure 13. Therefore one can finally

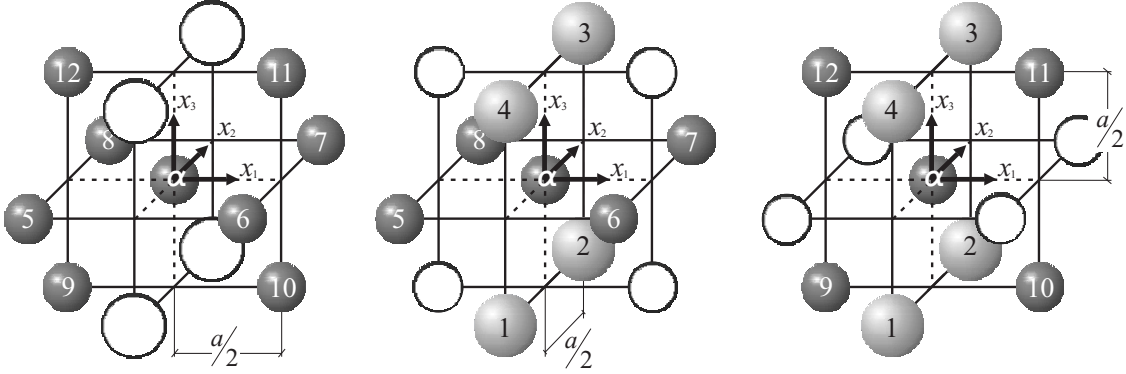


Figure 13: The number of atoms with a contribution in x_1 , x_2 and x_3 direction (the unfilled atoms have no contribution in the considered direction).

find for the elastic constants:

$$C_{111} = \Xi_a + \Xi_b \quad , \quad C_{112} = \frac{1}{2} \Xi_a + \Xi_b \quad , \quad C_{2323} = \frac{1}{2} \Xi_a \quad (129)$$

with the definitions:

$$\Xi_a = \frac{a^4}{\Omega_0} [\phi''(R^2) + 2F'(\bar{\rho}_e) \rho''(R^2)] \quad , \quad \Xi_b = 16 \frac{a^4}{\Omega_0} F''(\bar{\rho}_e) \rho'(R^2) \rho'(R^2). \quad (130)$$

In the case of the average of the VOIGT shear modulus it follows ($a^4 = 4R^4$) that:

$$G = \frac{2}{5} \Xi_a = \frac{2a^4}{5\Omega_0} [\phi''(R^2) + 2F'(\bar{\rho}_e) \rho''(R^2)] = \frac{8}{5} \frac{\phi_e \gamma (\gamma - \beta)}{\Omega_0} \quad (131)$$

or:

$$G = \frac{24}{15} \frac{\Phi_e \gamma (\gamma - \beta)}{\Omega_0}. \quad (132)$$

In the same manner one can show for the compressibility: $\kappa = \frac{2}{3} \Xi_a + \Xi_b$.

We now consider the vacancy formation energy E_{uvf} . For this purpose we want to follow the strategy of R.A. Johnson in [3] and note according to Eq (80) for equilibrium:

$$E_{\text{uvf}} = -6\phi_e - 12F(\bar{\rho}_e) + 12F\left(\frac{11}{12}\bar{\rho}_e\right) =$$

$$\stackrel{(77)}{=} -\Phi_e + 12(E_{\text{sub}} + \Phi_e) - 12E_{\text{sub}} \left[1 + h\left(\frac{11}{12}\right) \right] \exp\left[-h\left(\frac{11}{12}\right)\right] - 12\Phi_e \left(\frac{11}{12}\right)^{\frac{\gamma}{\beta}} \quad (133)$$

with $h(x) = \alpha \left(\sqrt{1 - \frac{1}{\beta} \ln x} - 1 \right)$. Performing a TAYLOR-expansion of the form:

$$h(x) = -\frac{1}{2} \frac{\alpha}{\beta} (x-1) + \frac{1}{4} \frac{\alpha}{\beta} \left(1 - \frac{1}{2\beta}\right) (x-1)^2 + \dots, \quad (134)$$

$$\exp[-h(x)] = 1 + \frac{1}{2} \frac{\alpha}{\beta} (x-1) - \frac{1}{4} \frac{\alpha}{\beta} \left(1 - \frac{1}{2\beta} - \frac{\alpha}{2\beta}\right) (x-1)^2 + \dots, \quad (135)$$

$$x^{\frac{\gamma}{\beta}} = 1 + \frac{\gamma}{\beta} (x-1) + \frac{1}{2} \frac{\gamma}{\beta} \left(\frac{\gamma}{\beta} - 1\right) (x-1)^2 + \dots. \quad (136)$$

An evaluation of these series at $x = \frac{11}{12}$ results in:

$$E_{\text{uvf}} = \frac{E_{\text{sub}}}{24} \left(\frac{\alpha}{\beta}\right)^2 \left[\frac{337}{1152} + \frac{1}{2304} \beta^2 \left(\frac{1}{2} + \frac{\alpha}{2}\right) \right] + \Phi_e \left(\frac{\gamma - \beta}{\beta}\right) \left(1 - \frac{1}{24} \frac{\gamma}{\beta}\right). \quad (137)$$

The various contributions in this equation can be also investigated by means of quantum mechanical methods. Following Johnson in [3] the leading term of Eq (137) is $\Phi_e \left(\frac{\gamma - \beta}{\beta}\right)$. Therefore it is reasonable to consider the approximation:

$$E_{\text{uvf}} \cong \Phi_e \left(\frac{\gamma - \beta}{\beta}\right). \quad (138)$$

Acknowledgements It is a pleasure to acknowledge the hospitality and the stimulating and friendly discussions with the members of the department for elasticity theories (mechanical-mathematical faculty) from the Moscow Lomonosov State University, Russia. Further the research was supported by the scholarship program of the German Federal Environmental Foundation.

References

- [1] Dreyer, W., Müller, W.H.: Toward Quantitative Modeling of Morphology Changes in Solids with Phase Field Theories: Atomistic Arguments for the Determination of Higher Gradient Coefficients. Key Engineering Materials **Vols 240-242**, ©Trans Tech Publications, Switzerland, 113–126 (2003)
- [2] Dreyer, W., Müller, W.H.: A study of coarsening in tin/lead solders. International Journal of solids and Structures **Vol 37**, 3841–3871 (2000)
- [3] Johnson, R.A.: Analytic nearest-neighbor model for fcc metals. Physical Review B **Vol 37**, 3924–3931 (1988)

- [4] Johnson, R.A.: Relationship between Two-Body Interatomic Potentials in a Lattice Model and Elastic constants. *Physical Review B* **Vol 6**, 2094–2100 (1972)
- [5] Johnson R.A.: Relationship between two-body interatomic potentials in a lattice model and elastic constants. II. *Physical Review B* **Vol 9**, 1304–1308 (1974)
- [6] Cahn, J.W., Hilliard, J.E.: Free Energy of a Nonuniform System. I. Interfacial Free Energy. *The Journal of Chemical Physics* **Vol 28(2)**, 258–267 (1958)
- [7] Cahn, J.W.: Spinodal Decomposition. *Transactions of the Metallurgical society of AIME* **Vol 242**, 166–180 (1968)
- [8] Langer, J.S.: Theory of Spinodal Decomposition in Alloys. *Annals of Physics* **Vol 65**, 53–86 (1971)
- [9] Binder, K.: Spinodal Decomposition. In: Haasen, P. (ed.) *Material Science and Technology*, Vol. 5, Phase Transformation in Materials, 405–471. VCH Verlagsgesellschaft Weinheim, (1990)
- [10] Hecht, U., et al.: Multiphase solidification in multicomponent alloys. *Materials Science and Engineering* **Vol R46**, 1–49 (2004)
- [11] Dreyer, W., Wagner, B.: Sharp-interface model for eutectic alloys Part I: Concentration dependent surface tension. *Interfaces and Free Boundaries* **Vol 7**, 199–227 (2005)
- [12] Daw, M.S., Baskes, M.I.: Semiempirical, Quantum Mechanical Calculation of Hydrogen Embrittlement in Metals. *Physical Review Letters* **Vol 50**, 1285–1288 (1983)
- [13] Daw, M.S., Baskes, M.I.: Embedded-atom method: Derivation and application to impurities, surfaces and other defects in metals. *Physical Review B* **Vol 29**, 6443–6453 (1984)
- [14] Rose, J.H., Smith, J.R., Guinea, F., Ferrante, J.: Universal features of the equation of state of metals. *Physical Review B* **Vol 29**, 2963–2969 (1984)
- [15] Winter, M.: WebelementsTM, University of Sheffield, <http://www.webelements.com>
- [16] Duderstadt, F.: Anwendung der von Kármán’schen Plattentheorie und der Hertz’schen Pressung für die Spannungsanalyse zur Biegung von GaAs-Wafern im modifizierten Doppelringtest. *PhD-thesis*. Technical University Berlin, Faculty V (2003)
- [17] de Fontain, D.: Clustering Effects in Solid Solutions. In: Hannay, N.B. (ed.) *Treatise on Solid State Chemistry*, **Vol 5 - Changes of State**, Plenum Press New York, 129–178 (1975)
- [18] MTDData NPL Databank for Materials Thermochemistry. National Physical Laboratory, Queens Road, Teddington, Middlesex, TW11 0LW (1998)
- [19] Johnson R.A.: Alloy model with the embedded-atom method. *Physical Review B* **Vol 39**, 12554–12559 (1989)
- [20] Kittel, C.: Einführung in die Festkörperphysik (3. erweiterte und verbesserte Auflage). R. Oldenbourg Verlag München Wien, John Wiley & Sons GmbH, Frankfurt (1973)
- [21] Liu, I-S.: Method of Lagrange Multipliers for Exploitation of the Entropy Principle. *Archive for Rational Mechanics and Analysis* **Vol 46**, 131–148 (1972)

- [22] Najafabadi, R., Srolovitz D.J., et al.: Thermodynamic properties of metastable Ag-Cu alloys. *Journal of Applied Physics* **Vol 74 (5)**, 3144–3149 (1993)
- [23] Feraoun, H., et al.: Development of modified embedded atom potentials for the Cu-Ag system. *Superlattices and Microstructures* **Vol 30 (5)**, 261–271 (2001)
- [24] Baskes, M.I.: Modified embedded-atom potentials for cubic materials and impurities. *Physical Review B* **Vol 46**, 2727–2742 (1992)
- [25] Lee, B.-J., Baskes, M.I., Kim, H., Cho, Y.K.: Second nearest-neighbor modified embedded atom method potentials for bcc transition metals. *Physical Review B* **Vol 64**, 184102-1–184102-10 (2001)
- [26] Pasianot, R., Savino, E.J.: Embedded-atom-method interatomic potentials for hcp metals, *Physical Review B* **Vol 45**, 12704–12710 (1992)
- [27] Küpper, M., Masbaum, N.: Simulation of particle growth and Ostwald ripening via the Cahn-Hilliard Equation. *Acta Metallurgica et Materialia* **Vol 42 (6)**, 1847–1858 (1994)